GEOTECHNICAL ENGINEERING PROJECT DAY 2017

A Presentation of Best Geotechnical Engineering Undergraduate Projects in Sri Lankan Universities

August 30, 2017
At IESL Auditorium

Organised by the
SRI LANKAN GEOTECHNICAL SOCIETY

SLGS

GEOTECHNICAL ENGINEERING
PROJECT DAY – 2017

Message from the President - SLGS

From its inception, Sri Lankan Geotechnical Society has provided a forum for disseminating new knowledge in the field of geotechnical engineering and promoting research. It has organized many conferences, workshops and field visits in this context.

The Project Day competition is an annual event held among Sri Lankan undergraduates doing projects in the field of geotechnical engineering. It commenced in year 2000 with the objective of encouraging them to do good research and publish. Participants are expected to present their findings in a concise four paged paper and make a 15 minute oral presentation. The best paper and the second paper will receive cash awards and certificates.

Many winners in the past years have proceeded to do higher studies and established good carriers in the field of Geotechnical Engineering as both academics and practicing engineers.

It is encouraging to note that there are fourteen papers on a wide variety of topics this year. I thank all the authors for their interest and commitment and hope they will continue with the habit of presenting their research in written form. It is only when one starts to write his findings he would realize the gaps in his work or knowledge and would be able to rectify them.

I also wish to convey my sincere gratitude to the panel of evaluators; Emeritus Professor B. L. Tennekoon, Prof. H. S. Thiakasiri and Dr. J. S. M. Fowze.

Prof. Athula Kulathilaka
President – SLGS

CONTENTS

Finite Element Analysis on the Effect of Deep Embedded Retaining Structures on the Settlement of Raft Foundations

M.P. Amarasinghe
Department of Civil Engineering, University of Moratuwa, Sri Lanka

ABSTRACT: Most of the foundation designs are conservative, as the failure in foundation will result in failure of the structure. The effects of presence of deep embedded retaining walls on the settlement characteristics of raft foundations have been investigated to find out whether the effect from embedded retaining walls can be used for an economical design. With an intention to investigate on that behavior, a numerical analysis based on FEM using Plaxis 2D software and an experiment on a scaled model was carried out, as the field experiments are expensive, complex and time consuming. The behavior of stress and load with the depth of embedment and the distance to the retaining wall from footing edge was investigated. In the scaled model for both experimental and finite element methods, the stress corresponding to 25mm settlement increased with the depth of embedment and decreased with the increase of the gap between the wall and the foundation. But in computer simulation of raft confined by a deep embedded retaining wall no such variation was observed. It was concluded that this was due to the change in mode of bearing capacity failure of shallow foundations as the size of foundation changes.

1 INTRODUCTION

Foundations are used to transfer the loads of structures to the ground. A good foundation design can extend the lifetime of a structure. Raft foundation is a concrete slab extended over a large area reducing the contact pressure supporting many concrete columns, beams and slabs, widely used in constructing buildings with basements. Often excavation of great depths is required for raft foundation construction therefore support from embedded retaining walls is required.

Embedded retaining walls are used in many civil engineering applications for embankment stabilization, basement constructions, in underground passes and for waterfront projects. Embedded retaining walls obtain lateral support from penetrating into the ground and may also be supported by structural members. During early days embedded retaining walls were constructed of either soldier piles or steel sheet piles. Later concrete walls were formed using various techniques such as slurry trenches, contiguous or secant piles and diaphragm walls (Dong, 2014).

The purpose of this research is to analyze the effect of presence of deep embedded retaining structures for the settlement characteristics of a raft foundation using finite element techniques. When designing a shallow foundation the bearing capacity and the settlement of it have to be considered. Settlements can either be immediate or consolidation according to (Terzaghi, Peck and Mesri, 1996). Not much is known on the effect of deep embedded structures on settlement of raft. It is planned to analyze and identify the relationship between load/stress immediately below the footing (for a specific settlement of footing) with the change in depth of embedment of retaining wall, and the distance to the retaining structure from footing edge if the raft is confined by a deep embedded retaining wall.

2 OBJECTIVES

Objectives are to investigate experimentally, the effect of deep embedded retaining structures on the settlement of raft foundation using a model. Then obtain results by numerical modeling of a shallow foundations confined by a deep embedded retaining structure and propose recommendations on the strength enhancement and settlement reduction of shallow foundations due to the presence of deep embedded retaining structures.

3 METHODOLOGY

- After conducting a thorough literature review an experimental procedure was adopted using a model shallow foundation confined by a deep embedded retaining wall.
- Then for the experimental scaled model a numerical analysis based on finite element analysis was carried out using computer software Plaxis 2D.

- Results were compared and verified with experimental results.
- Next by computer simulation of a raft confined by a retaining structure results were obtained.

3.1 *Experimental Procedure*

An experimental procedure using a scaled model of a shallow foundation confined by a deep embedded retaining wall was used. Two timber boxes of 300mmx300mm and 500mmx500mm of height 600mm were used as the retaining wall. A timber plate of 200mmx200mm was used as the raft foundation. A large container was filled with sand after placing the timber box at required depth of embedment and filled to a height of 600mm outside the box and in inside with a layer of 400mm from the bottom. In filling the container the falling height of sand was kept constant to keep the density of sand uniform.

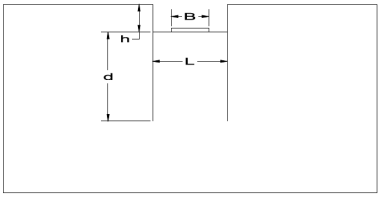

Figure 1: Experimental setup

Table 1 : Summary of the experimental procedure

Width of the timber box	Depth of embedment (d)	Depth of excavation (h)	Width timber footing (B)
300mm	100mm	200mm	200mm
	200mm		
	300mm		
500mm	100mm	200mm	200mm
	200mm		
	300mm		

Table 1 summarizes the scenarios in the experiment. Timber plate was kept at the centre of the box. Because of the practical difficulty in placing the dial gauge few steel plates were first kept on the plate as loads and then using hydraulic jacks those plates were loaded.

Number of divisions proving ring deflected for every 2mm deflection in dial gauge was measured and converted to a force using calibration data. As there is an initial settlement due to the load from steel plates that load and settlement must be added to the load and deflection. Therefore the mass of the steel plates, hydraulic jack and timber plate were measured and graphically calculated the load that would result in a 25mm settlement assuming the settlement –load curve to be linear for small settlement values as observed in researches of (Leong and Huat, 2013)) and (Unsever, Matsumoto and Ozkan, 2015). The soil unit weight was calculated using the proctor mold. Proctor mold was filled with sand at the same height that the container was filled and the mass of sand that occupied the proctor mold was measured and dry weight was calculated.

3.2 *Numerical Analysis*

The experimental procedure was modeled using Plaxis 2D Finite element software. Considering the symmetry only a half of the geometry was modeled. For this analysis axisymmetric model with 15 node triangular elements was selected. Boundaries were placed at sufficiently remote distances so that no restrains or constrains were present for the movement in area considered.

For this a circular raft footing of radius ‘r’ and excavation area of radius ‘R’ was used where the area of plate and area excavated are same as in the experiment. For different depths of embedment ‘d’, and for different ‘R’ values at excavation depth of ‘h’ required stress at the bottom of the raft footing to cause a prescribed settlement of 25mm was generated. Updated mesh analysis was carried out as the displacements are larger compared to the dimensions of the model.

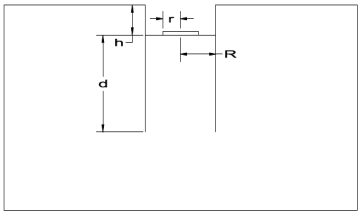

Figure 2: Scaled model for numerical analysis

Table 2 : Cases of numerical analysis on model

Size of the timber box that is being modeled	(R) mm	(h) mm	(d) mm	(r) mm
300mm*300mm	169.8	100	200	112.8
		200		
		300		
500mm*500mm	282.1	100	200	112.8
		200		
		300		

Then a numerical analysis was carried out using computer simulation of a raft foundation confined by a deep embedded retaining wall based on finite element method. For this a raft of size 20mx20m was used. For a prescribed displacement of 50mm the stress immediately below the raft footing was obtained, changing the length of wall to 21m, 22m, 24m and 26m and for the depth of embedment 3m, 6m, 9m and 12m. The raft foundation confined by deep embedded retaining wall was analysed with a

plane strain model and 15 node elements were utilized. Half of the model was used due to its symmetry about y axis. Boundaries were placed at sufficiently remote distances so that no restrains or constrains were present for the movement in area considered.

4 RESULTS AND DISCUSSION

4.1 *Experimental results*

After obtaining the readings from the experiment, a correction for pre loading was done using a graphical system. Then stress corresponding to 25mm settlement was found using Figs 3 & 4. Fig 5 presents the relationship between stress at 25mm settlement and the depth of embedment for the two timber boxes. It was observed that the stress at 25mm increase with the depth of embedment. The relationship of stress at 25mm settlement and the distance to the wall from plate edge was obtained varying the depth of embedment. Results are presented in Figs 6 & 7 where the stress increases with the depth & decreases with the distance to the wall respectively.

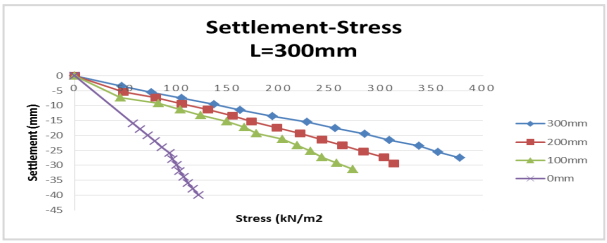

Fig 3: Settlement-Depth of embedment for L=300mm

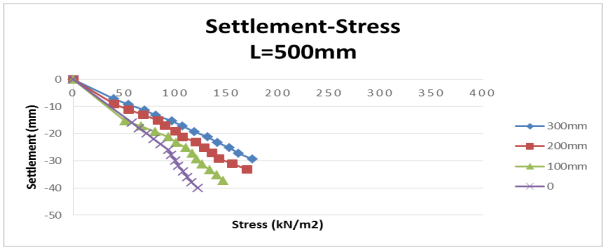

Fig 4: Settlement-Depth of embedment for L=500mm

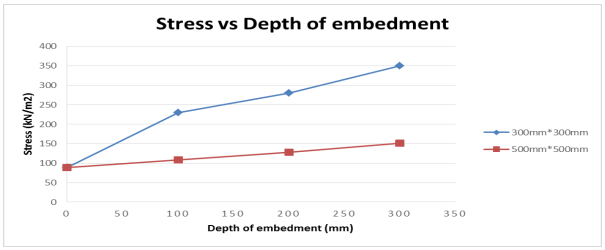

Fig 5: Stress vs Depth of embedment

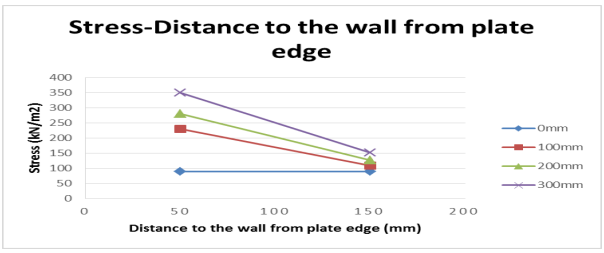

Fig 6: Stress at 25mm settlement-gap between wall and plate

4.2 *Numerical analysis results*

From numerical analysis on the small scale model it was observed that relationship between stress at 25mm and depth of embedment vary similar to the experimental results for the two different R values compared in Figs 7 & 8. When the plate is closer to the wall it shows a great increase in load at 25mm settlement for the same depth of embedment as shown in Fig 9.

In the computer simulation of a proto type scale raft confined by a deep embedded retaining wall it was observed that there is no significant change in stress at 50mm settlement with the depth of embedment and distance to the wall from raft edge as shown in curves in Figs 10 & 11 respectively. When checked if there is any change in stress with depth of embedment for different Young's modulus values of soils no significant change observed.

It was observed that the maximum stress immediately below foundation occurs at the center and smaller at edge similar to ground settlement in excavation stated in Wu, Ou, & Tung, (2010). The average of the stress below the foundation was obtained as the stress at prescribed settlement.
A 2D model for the numerical analysis was used where the corner effect was neglected. Corner effect is the effect of wall deformation and ground movements being smaller close to the wall corner than around the wall center according to (Wu, Ou and Tung, 2010) and (Ou, Chiou and Wu, 1996). A 3D analysis required to identify this effect.

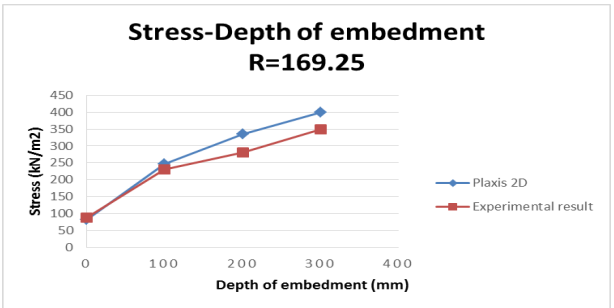

Fig 7: Stress-depth of embedment for R=169.25mm

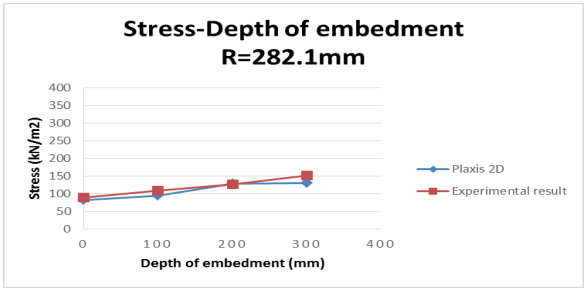

Fig 8: Stress-depth of embedment for R=282.1mm

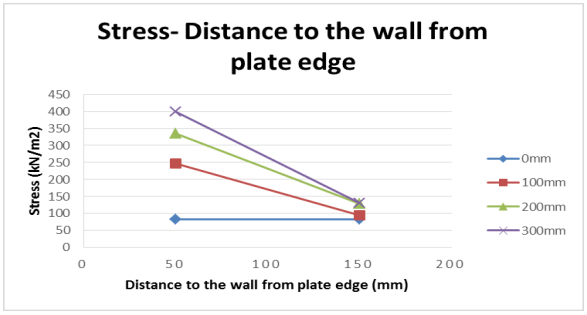

Fig 9: Stress at 25mm settlement- gap between wall and plate

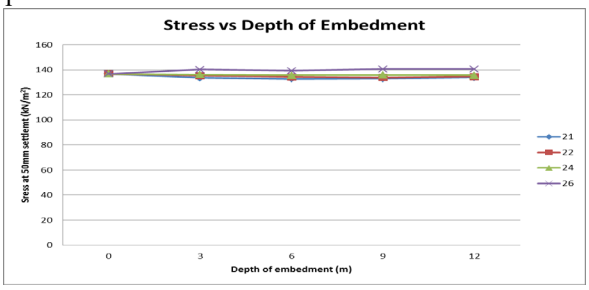

Fig 10: Stress-depth of embedment

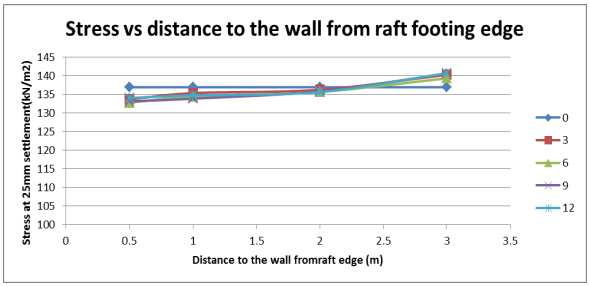

Fig 11:Stress vs Distance to the wall from raft footing edge

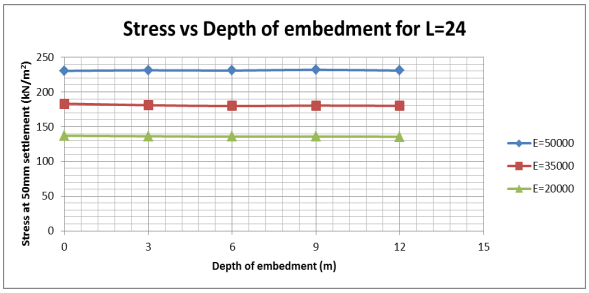

Fig 12: Stress- depth of embedment for different elasticity of soils

5 CONCLUSION

In this study, the effects of presence of deep embedded retaining walls on the settlement characteristics of raft foundations have been investigated. An experiment was carried out on a scaled model and the results were verified using numerical analysis based on finite element method. It was observed that the stress corresponding to 25mm settlement increases with the depth of embedment and when the wall is closer to the raft foundation.

In computer simulation of a raft confined by deep embedded retaining wall no such variation with depth or with the gap between wall and footing was observed. It can be concluded that this behavior is due to change in the mode of bearing capacity failure of shallow foundations on sand. Scaled model shows a general shear failure mode while computer simulation of an actual application shows a punching shear failure due to the size of the foundation. The reason for the decrease in load at 25mm settlement as the gap increase is the effect of embedded wall on the slip surface and on stress bulb. As the gap increased the effect was minimized.

It can be concluded that for small footings confined with a deep embedded retaining wall the capacity against settlement failure of the soil can be increased. But for large footings or when the gap between footing edge and retaining wall is high this won't be valid.

6 REFERENCE

Dong, Y. (2014) *Advanced Finite Element Analysis of Deep Excavation Case Histories*. University of Oxford.

Leong, T. K. and Huat, C. S. (2013) 'Sustainable design for unpiled-raft foundation structure', in *Procedia Engineering*, pp. 353–364. doi: 10.1016/j.proeng.2013.03.032.

Ou, C.-Y., Chiou, D.-C. and Wu, T.-S. (1996) 'Three-Dimensional finite element analysis of deep excavations', *Journal of Geotechnical Engineering*, 122(May), pp. 337–345. doi: 10.1061/(ASCE)0733-9410(1996)122:5(337).

Terzaghi, K., Peck, R. B. and Mesri, G. (1996) 'Soil Mechanics in Engineering Practice, Third Edition', *Wiley-Interscience Publication, John Wiley and Sons, Inc.*, p. 664 pp. doi: 10.1016/S0013-7952(97)81919-9.

Unsever, Y. S., Matsumoto, T. and Ozkan, M. Y. (2015) 'Numerical analyses of load tests on model foundations in dry sand', *Computers and Geotechnics*, 63, pp. 255–266. doi: 10.1016/j.compgeo.2014.10.005.

Wu, C. H., Ou, C. Y. and Tung, N. (2010) 'Corner effects in deep excavations-establishment of a forecast model for taipei basin T2 zone', *Journal of Marine Science and Technology*, 18(1), pp. 1–11.

Compressibility Characteristics of Residual Soil

V.G.D. Gangani
Department of Civil Engineering, University of Moratuwa, Sri Lanka

Abstract: Sri Lankan residual soils are formed by weathering of metamorphic rock. Residual soil and sedimentary soil distinguish different behavioral, compositional and structural characteristics mainly due to the variations in soil formation process, structure and mineralogy. Consolidation tests were carried out to identify the compressibility characteristics of residual soils in Sri Lanka. Both Rowe cell and Oedometer were used for the experiments. Rate and magnitude of consolidation is predicted by determining coefficient of consolidation (C_v), compression index (C_c) & coefficient of volume compressibility (m_v). Taylor's method, Casagrande method, velocity method and pore water pressure readings were used to find coefficient of consolidation relevant to the test results.

1. INTRODUCTION

Identifying the behaviour of soils is the fundamental and most significant component in any construction work. Despite of the fact whether it is a sedimentary soil or a residual soil, the geotechnical properties of a subsoil affected by proposed construction has to be well known prior to any design.

Sri Lanka being a tropical country metamorphic originated residual soil is abundantly available. The subject of soil mechanics was developed in countries with sedimentary soils. Hence, almost all the geotechnical concepts have been developed considering only the characteristics of sedimentary soils. Residual soils had not been identified as a separate soil type or treated separately. The concepts applied to sedimentary soils are extended and applied to residual soils as well.
Most of the differences in residual soils and sedimentary soils occur due to their different formation processes. Most correctly the sedimentary soils are undergoing additional processes like erosion, transportation, compaction due to self-weight, secondary consolidation, etc. The hierarchy in **Figure 1** (Wesley, 2009) shows the formation processes of the two soil types.

When homogeneity of the two soil types is considered sedimentary soils tend to be more homogeneous than residual soils. This is due to the sorting process occurring during transportation and deposition of weathered soil particles. Residual soils do not experience these methodical sorting processes, hence they tend to be much heterogeneous than sedimentary soils.

A stress history is created by either a constant stress state which is applied over a period of time or a change in the direction of the stress path. During the formation process of sedimentary soil loading, unloading and reloading may occur resulting a stress history. So a virgin consolidation line can be identified for sedimentary soils. This is the premier factor in identifying the over consolidated and normally consolidated soils. The above discussed concepts, stress history, virgin consolidation line, over consolidation and normal consolidation are not applicable to residual soils.

Absence of the above mentioned homogeneity and stress history makes residual soils more complex and difficult to analyze. This makes the applicability of conventional theories to analyses of residual soils questionable.

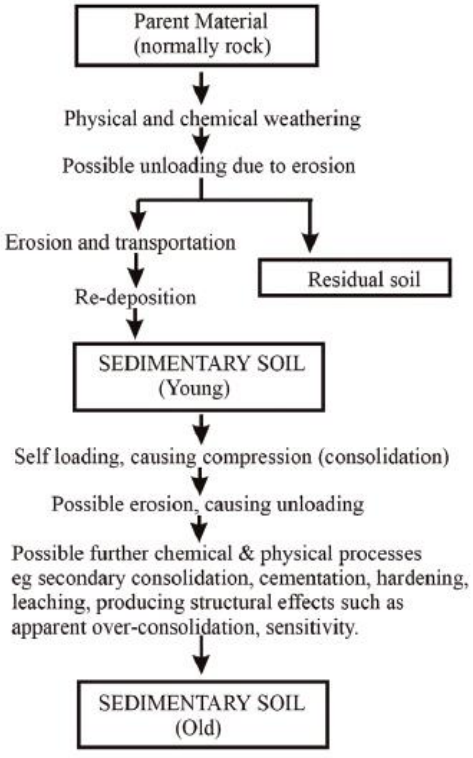

Figure 1: Soil formation process
(After Wesley, 2009)

2. METHODOLOGY

There are several methodologies that had been used to determine the compressibility characteristics of residual soil. Prediction of the magnitude and rate of settlement is done by carrying out experiments to determine the desired parameters such as coefficient of consolidation (C_v), compression index (C_c) & coefficient of volume compressibility (m_v). In order to determine above components, settlement and time readings should be analyzed using a relevant approach. In most of the past studies, consolidation test results were analyzed using Terzaghi's one dimensional consolidation model.

Oedometer test is the experimental approach proposed by Terzaghi which is most commonly known as Consolidometer test. Soil specimens of 20 mm thickness are subjected to vertical loading under doubly drained condition. Therefore we can only predict settlements of soils under wide surface load over a thin compressible layer where the effects of lateral pore pressure dissipation can be neglected.

Rowe cell apparatus has significant advantages over the conventional Oedometer. Usually properties of residual soils are varying vastly within a small area and the representativeness of oedometer sample has become questionable. Since Rowe cell apparatus accommodates much larger samples to be tested, adopting Rowe cell would be an acceptable solution for the matter of representativeness. The Rowe cell used for this study accommodates 50 mm thick samples with 75 mm diameter. The major advantage is the ability of measuring pore water pressure in the sample. This will indicate the end of consolidation process and can be used to find coefficient of consolidation as well.

For this research on residual soils, both Rowe cell and Oedometer were used appropriately to identify the effect of sample thickness and drainage path for consolidation.

2.1 Experimental Programme

Tests were done on both undisturbed samples and remoulded samples of residual soils in which particles greater than 5 mm in size were removed. Initially remoulded sample was prepared at a water content of 65% which is greater than liquid limit to ensure saturation. The second series of tests were done after compacting the soil at optimum water content and making it fully saturated. A third series of tests were done on a saturated natural soil sample without removing coarse particles.

Both Rowe cell and Oedometer cell were filled with the sample maintaining same density for a better comparison. In both tests 24 hr long loading increments were adopted. In the Rowe cell, pore water pressures were completely dissipated much earlier than 24 hrs. Settlement readings were taken in both loading and unloading stages.

2.2 Analysis of test results

2.2.1. Rate of Consolidation (C_v)

Four methods were adapted to find the coefficient of consolidation in order to identify the settlement characteristics of the soil. Taylor's method, Casagrande method and velocity method (Parkin, 1978) were used to find C_v for each loading step. The pore water pressure measurements obtained by Rowe cell apparatus were used to find C_v with the aid of time factors defined by Terzaghi. Typical settlement plots drawn for sample 1 (remoulded sample with WC > LL) using the three methods are presented in **Figure 2, Figure 3 and Figure 4**.

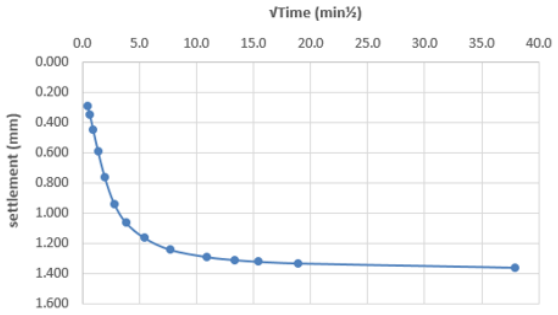

Figure 2: Taylor's method – Rowe cell sample1

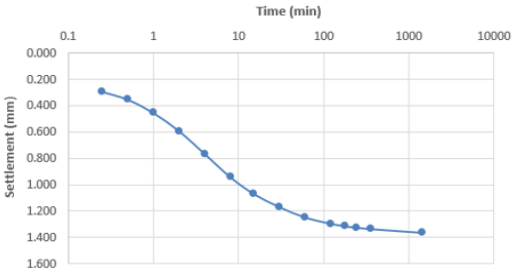

Figure 3: Casagrande method – Rowe cell sample1

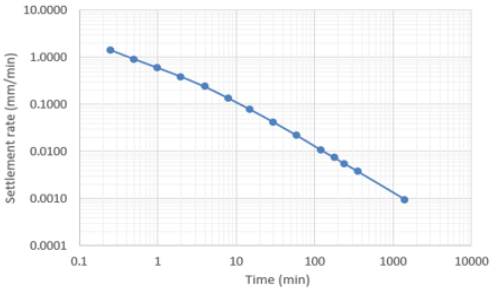

Figure 4: Velocity method – Rowe cell sample1

C_v values of sample 1 determined using the three graphical construction methods are shown in Figure 5 and Figure 6.

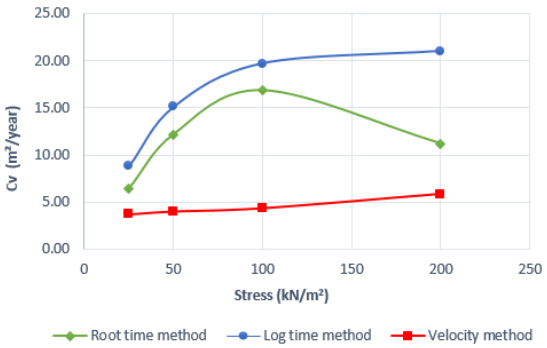

Figure 5: C_v of Oedometer sample 1

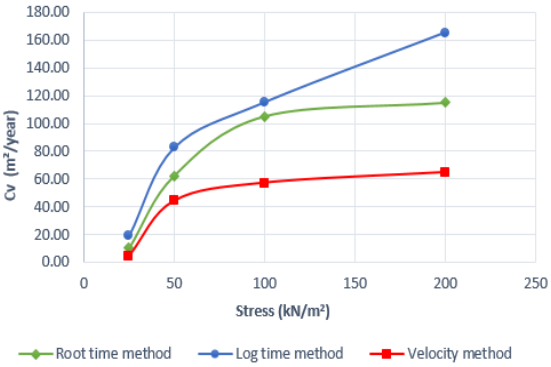

Figure 6: C_v of Rowe cell sample 1

In Rowe cell test, the pore water pressure values read by the pressure transducers were recorded with every settlement reading. The increase and dissipation of pore pressure could be clearly identified by graphically representing the pore pressures and settlements together. **Figure 7** (plotted in log scale) and **Figure 8** (plotted in linear scale) show that the consolidation settlement after pore water pressure dissipation is quite small.

Rowe cell represents single drainage consolidation and pore pressure measurements at the undrained boundary were used to calculate the coefficient of consolidation. The PWP increase caused by the application of the load is fully felt at the bottom level after a response time of several minutes. The calculated $C_v$values are presented in **Table 1**.

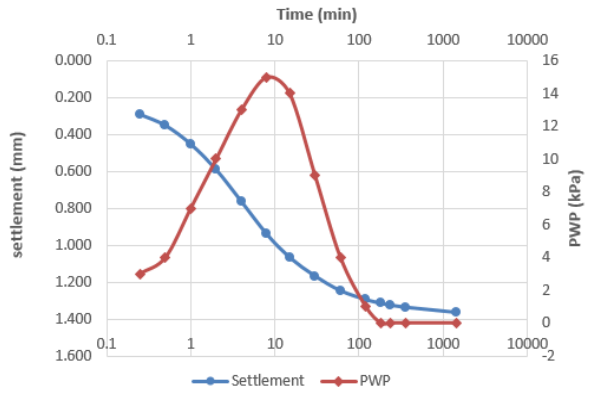

Figure 7: PWP & settlements plotted in log scale

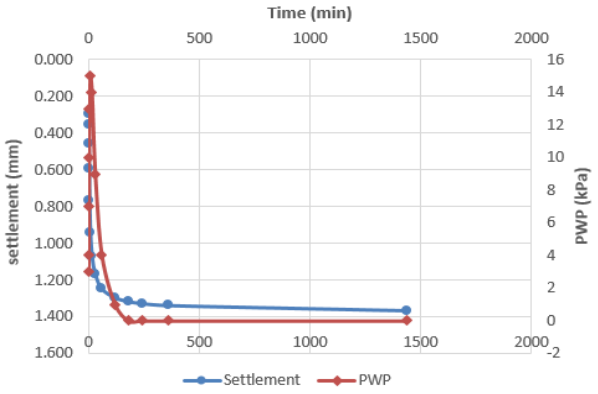

Figure 8: PWP & settlements plotted in linear scale

Pressure increment (kN/m2)	Δσ	u_o	Time (min)	u_z	U %	Tv	Cv (m²/year)
0 - 25	25	25	8	14	44	0.33	40.09
	25	25	15	13	48	0.36	23.32
	25	25	30	11	56	0.43	13.93
	25	25	60	10	60	0.46	7.45
	25	25	120	7	72	0.62	4.98
	25	25	180	5	80	0.75	4.05
	25	25	240	4	84	0.84	3.40
	25	25	360	3	88	0.92	2.48
25 - 50	25	25	8	10	60	0.46	55.88
	25	25	15	9	64	0.50	32.39
	25	25	30	5	80	0.75	24.30
	25	25	60	2	92	0.94	15.23
	25	25	120	1	96	0.97	7.86
50- 100	50	50	8	15	70	0.57	69.24
	50	50	15	14	72	0.62	40.17
	50	50	30	9	82	0.80	25.92
	50	50	60	4	92	0.94	15.23
	50	50	120	1	98	0.98	7.94
100 - 200	100	100	8	24	76	0.66	80.18
	100	100	15	22	78	0.70	45.35
	100	100	30	18	82	0.80	25.92
	100	100	60	15	85	0.85	13.77
	100	100	120	14	86	0.88	7.13
	100	100	180	13	87	0.90	4.86
	100	100	240	13	87	0.90	3.64
	100	100	360	12	88	0.92	2.48
	100	100	480	11	89	0.93	1.88
	100	100	1440	6	94	0.96	0.65

Table 1: C_v calculated by PWP values

These values gives an indication that C_v may not be a constant during a load increment. However there should be further studies to understand this effect.

2.2.2. Compressibility Coefficients

The compressibility of a soil is evaluated through the parameters; Coefficient of volume compressibility (m_v) and Compression index (C_c). These parameters were determined for the three types of samples. The concept of pre-consolidation pressure and the plot of e vs log σ are not relevant for residual soils(Wesley, 2010).Therefore more attention has placed on the Coefficient of volume compressibility.

Void ratio was plotted against pressure in both log scale and linear scale as shown in **Figure 8** and **Figure 9.**Compression index(C_c) were calculated using e vs log σ graph (**Table 2**).**Figure 10** shows the variation of m_v with the stress level for the three Oedometer samples.

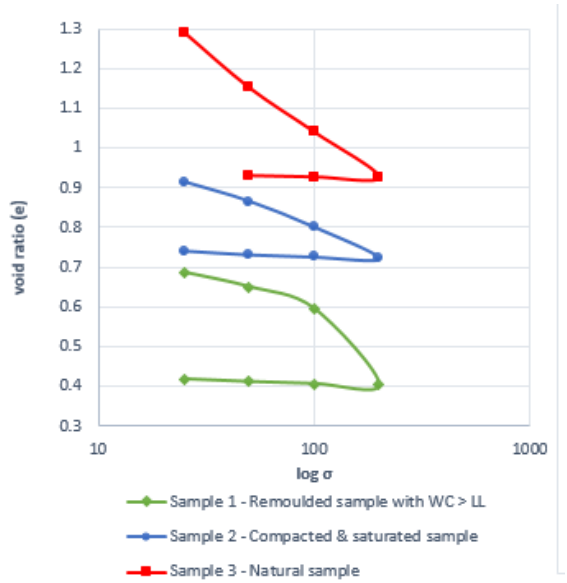

Figure 8: e vs log σ graphs for Oedometer samples

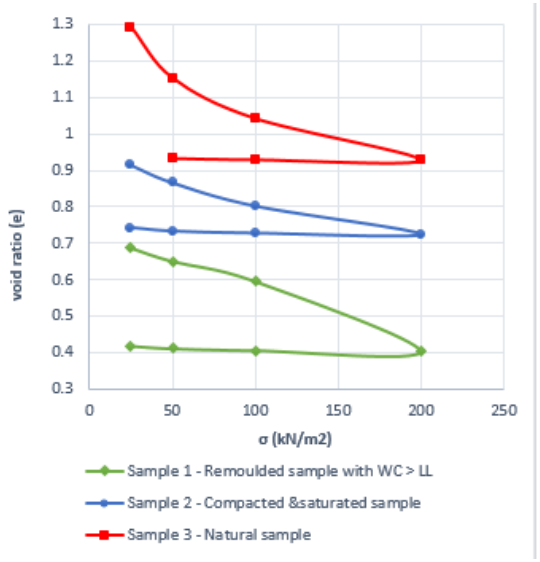

Figure 9: e vs σ graphs for Oedometer samples

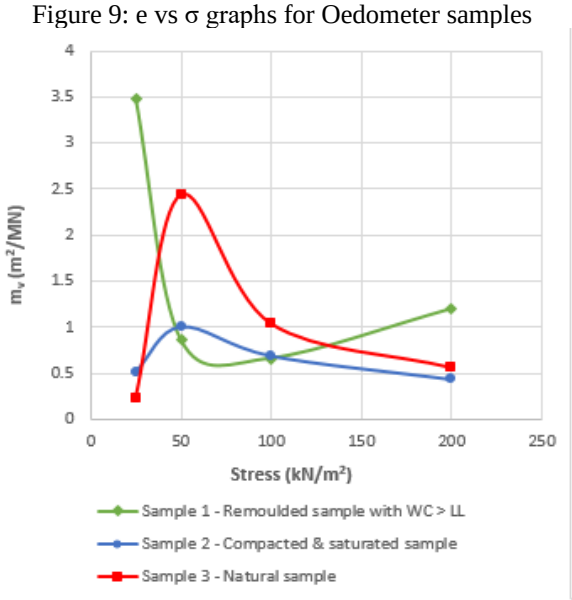

Figure 10: m_v vs stressgraphs for Oedometer samples

Table 2: C_c obtained by using e vs. log σ graphs

Sample	Cc	
	Oedometer	Rowe cell
Sample 1	0.670	0.210
Sample 2	0.270	0.003
Sample 3	0.420	0.203

3. CONCLUDING COMMENTS

The test results from Rowe cell has given higher C_v than Oedometer results. Rowe cell accommodates larger samples to be tested than in Oedometer. Therefore the larger sample represents higher rate at which the consolidation proceeds. This result can be linked with the conclusions of Tennakoon et al.(1986) which says that conventional methods of testing and analysis grossly under-estimates the rate of settlement. Rate of consolidation determined through the large samples, is more likely to represent field consolidation process. Therefore, Rowe cell can be recommended as a better option to predict rate and amount of consolidation settlements.

The graphs shown in Figure 8 and Figure 9 clearly indicates that the undisturbed soil sample(sample 3) has high void content than other samples. Both the remolded and compacted samples have consolidation curves lying well below that of the undisturbed sample. Effect of remolding has destroyed the soil structure and it has significantly influenced on the soil properties. Hence it can be said that the natural soil sample is highly structured and exists in a non-compact state(Wesley, 2010).

However it cannot be concluded that the Sri Lankan residual soils are highly structured and exists in a non-compact state, since only a very limited number of samples has been tested for this study. Further research should be done in order to give a better conclusion.

4. REFERENCES

1. Parkin, A. (1978). Coefficient of consolidation by the velocity method. *Geotechnique, Vol. XVIII*, pp. 472-474.

2. Tennakoon,B.L., Sivapatham,T., Kanagaratnam,S.P., Kuruppan,K. (1986). Consolidation characteristic of Residual clays in Sri Lanka. *Asian regional symposium on Geotechnical practices and Foundation Engineering.* Colombo.

3. Wesley, L. (2009). *Behaviour and geotechnical properties of residual soils and allophane clays.* Department of Civil and Environmental Engineering, University of Auckland, New Zealand.

4.Wesley, L. (2010). *Geotechnical Engineering in Residual Soils.* New Jersey: John Willey & Sons, Inc.

Shear Strength and Permeability Characteristic of Compacted Residual Soils in an unsaturated state

H.P.W.Dilanthi
Department of Civil Engineering, University of Moratuwa, Sri Lanka

ABSTRACT: Sloping grounds in Sri Lanka are formed of residual soils. During the periods of dry weather the ground water table is low and soils at upper levels of the slope are unsaturated and possess significant matric suctions. With prolonged rainfall and infiltration, matric suction will diminish to nearly zero. Perched water table can also be developed. Therefore, slopes that are stable in dry periods may fail when subjected to excessive rainfall. Soil Water Characteristic Curves (SWCC), Permeability function and shear strength parameters of unsaturated soil are essential parameters needed to model this behaviour. Vasanthan (2016) did a study for the first time in Sri Lanka to establish characteristics of an unsaturated soil (in an undisturbed state). But soil within the block samples was found to be quite variable. Therefore, this study was done on residual soils typically used to construct embankments. Residual soils are widely used for the construction of embankments and will be in an unsaturated state when compacted at OMC. This research focuses on the variation of shear strength with the matric suction and development of the permeability function of unsaturated residual soils compacted at optimum moisture content. Laboratory direct shear tests were done with a miniature tensiometer for the direct suction measurement. Permeability function for both wetting and drying phases were investigated. SWCC was also established from the test results. This research highlights the importance of these studies and presents the procedures that are being used.

1 INTRODUCTION

Residual soil formations encountered in Sri Lanka are derived from the weathering of metamorphic parent rock. Water table is deep and near surface soil is in unsaturated state and Pore water pressure (PWP) is negative especially during rainy seasons. This negative PWP contributes to additional shear strength of soil and stability of the slopes. Prolonged rainfall and infiltration can diminish matric suction to nearly zero. Perched water table or positive PWP can also be induced during heavy rainfall. This will frequently become a triggering factor for slope failures.

In order to understand the threshold values of rainfall leading to instability it is necessary to model this process with a reasonable accuracy. Vasanthan (2016) did a study for the first time in Sri Lanka to establish characteristics of an unsaturated soil (in an undisturbed state) derived from Southern expressway. The soil within the block sample of 0.3m x 0.3m x 0.3m was also found to be quite variable. Hence this study is done with a uniform soil typically used for construction of embankments. Residual soils are widely used for the construction of embankments and will be in an unsaturated state when compacted at OMC. In this project, soil sample for the testing was obtained by cutting a slope made of residual soil at university premises. Particles greater than 5mm were removed by sieving. Basic characteristics of these soils forming embankments such as; SWCC, Permeability function and unsaturated shear strength parameters are essential parameters in the analyses as these characteristics have not been established for typical residual soils used to construct embankments.

2 SUCTION MEASUREMENT

The matric suction in a soil is defined as;

$$S = U_a - U_w \quad (1)$$

Where u_a is the pore air pressure (equal to zero atmospheric condition) and u_w is the pore water pressure.

Jotisankasa et al. (2010) developed a miniature tensiometer at Department of Civil Engineering, Kasetsart University, Thailand. It consist of micro electro mechanical system (MEMs) pressure sensor, 1BAR High-Air-Entry porous ceramic and transparent acrylic tube. (Figure 1). This can be used to measure matric suction directly.

Fig.1 Miniature KU tensiometer sensor

3 ESTABLISHMENT OF BASIC SOIL CHARACTERISTICS

The particle size distribution determined by wet sieve analysis and hydrometer analysis is given in Fig 2.

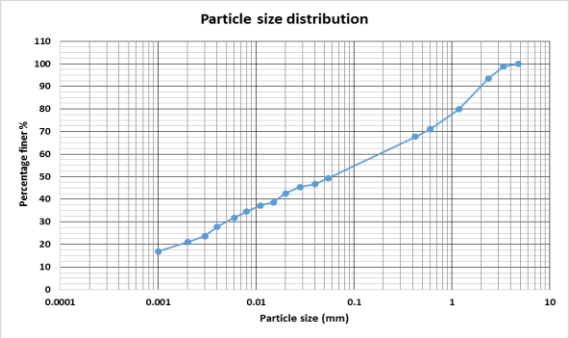

Fig. 2 Particle size distribution

Liquid Limit = 56%
Plastic Limit = 36%
Plasticity Index = 20%
Soil classification symbol = MH (according to Unified Soil Classification System)
Specific Gravity = 2.61
OMC = 23.10%
Maximum Dry Density = 1554 Kg/m^3

4 DETERMINING UNSATURATED SHEAR STRENGTH PARAMETERS

Shear strength of an unsaturated soil can be expressed as;

$$\tau = c' + (\sigma - u_a)\tan\phi' + c^s \quad (2)$$

Where, τ is shear stress at failure, c' is effective cohesion intercept, σ is normal total stress, u_a is pore air pressure (for atmospheric pressure, u_a equals zero), Φ' is the effective angle of shearing resistance, C^s is the additional cohesion in unsaturated soil due to matric suction, $(\sigma - u_a)$ is net normal stress at failure

The value of c^s can be determined as follows;

$$c^s = (u_a - u_w)\tan\phi_b \quad , \text{if } u_w < u_a \quad (3)$$

Where, Φ^b is angle of shearing resistance due to matric suction.

Direct shear tests were conducted on samples compacted at optimum moisture content. A minor modification was made to the top cap of conventional direct shear box, where a tensiometer is inserted through an opening of the top cap.

4.1 Tests to establish unsaturated Shear strength parameters

Tests were performed on approximately 92% saturated (as compacted) and fully saturated specimen . Variation of Shear stress with Shear strain and variation of Shear stress at failure vs Normal stress are given in Fig 3 and Fig 4 respectively.

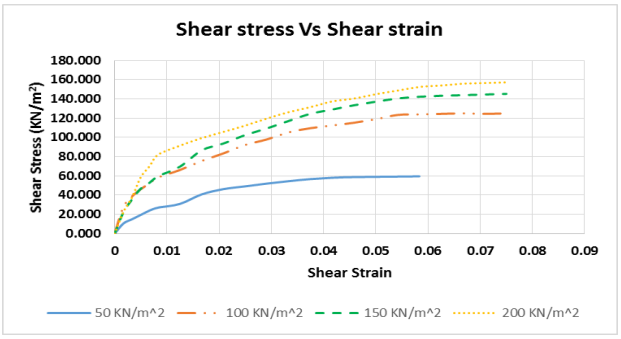

Fig. 3 The variation of shear stress with shear strain for approximately 92% saturated condition (as compacted)

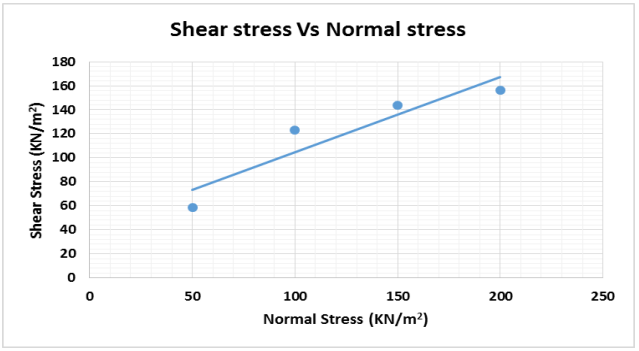

Fig 4: The variation of shear stress with normal stress for approximately 92% (as compacted) saturated condition

Variation of Matric suction during consolidating and shearing is given in Fig 5 and Fig 6 respectively

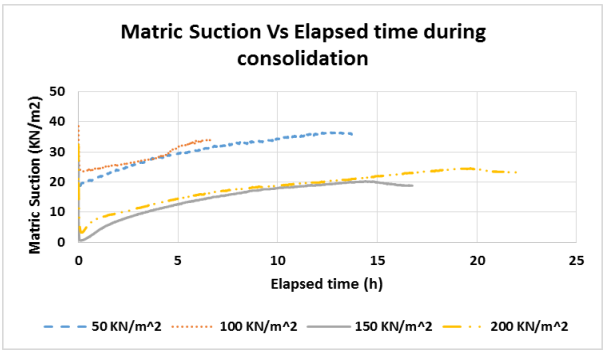

Fig. 5 The variation of matric suction with time at consolidation stage for approximately 92% saturated condition. (as compacted)

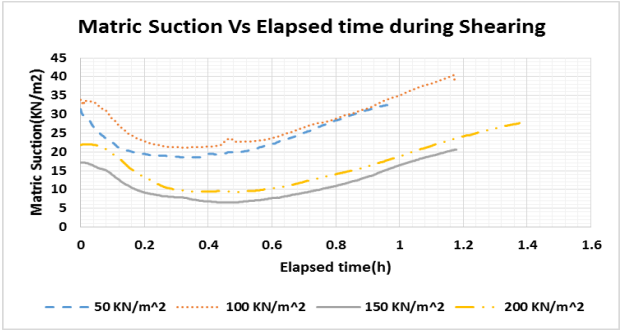

Fig. 6 The variation of matric suction with time at shearing stage for approximately 92% saturated condition. (as Compacted)

5 DETERMINAION OF SWCC AND THE PERMEABILITY FUNCTION

The values of suction at 3 locations can be used to calculate the hydraulic gradient, i, given by,

$$i = \frac{d(z - s/\gamma_w)}{dz} \quad (4)$$

Where z is the elevation head of each tensiometer relative to the base of sample, s is matric suction, and γ_w the unit weight of water.

As the quantity of flow is very small, the plot of change in soil mass was used to calculate the discharge velocity, v, at any particular time is given by;

$$v = \frac{dV_w}{A.\,dt} \quad (5)$$

Where dV_w is the change of volume of water in soil sample which can be calculated from change in soil mass during test, *A* is the cross section area of sample, and dt is the elapsed time.

The value of permeability at any suction and volumetric water content can then be calculated by equation 6. (Jotisankasa, et al 2010)

$$k = {}^{v}/_{i} \quad (6)$$

Fig.7 Testing procedure for continuous Measurements

5.1 Tests to establish SWCC and Permeability function by using continuous measurement.

Tests were conducted to determine SWCC and permeability function on the drying path and wetting path with continuous measurements.

Matric suction variation with time is plotted for both drying and wetting tests. Drying path tests were conducted by allowing a saturated sample to dry under atmospheric conditions. The dried sample was wetted by applying drops of water through a burette in the wetting path test.The results of drying test are presented in Figures 8. Wetting test results are presented in Figures 9.

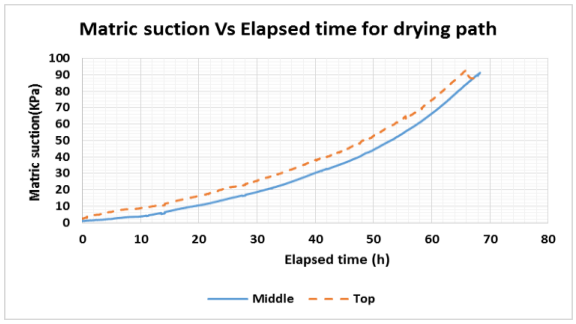

Fig.8 Matric suction variation with time for drying path

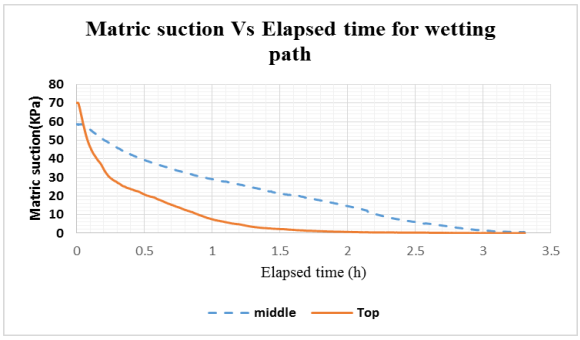

Fig.9 Matric suction variation with time for wetting path

The hydraulic gradient was estimated using Equation 3 for both drying and wetting test. The results are presented in Figure 10 & 11

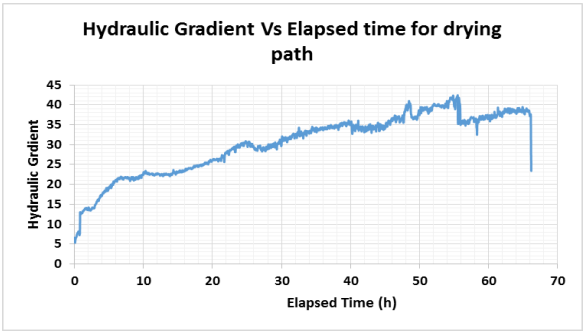

Fig. 10 Hydraulic gradient Vs time for drying path

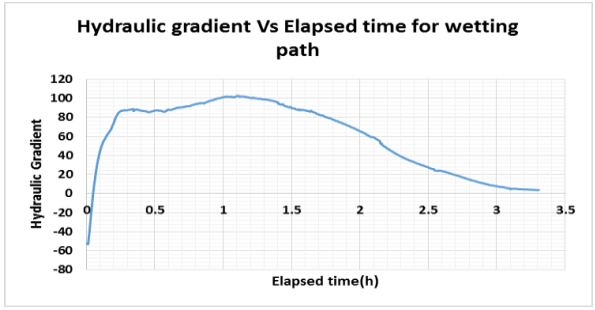

Fig. 11 Hydraulic gradient Vs time for wetting path

The hydraulic conductivity was estimated using Equation 5. Results are presented in Figure 12 & 13.

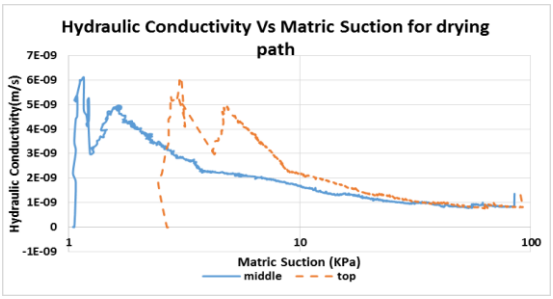

Fig. 12 Hydraulic conductivity variation with Matric suction for drying path

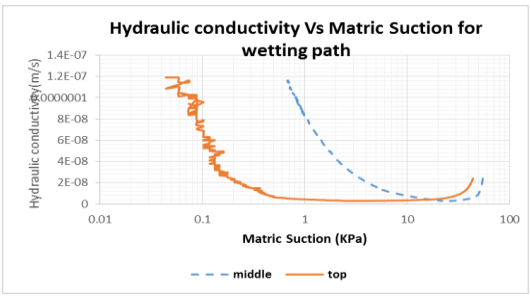

Fig. 13 Hydraulic conductivity variation with Matric suction for wetting path

6 ESTABLISHMENT OF SWCC USING KU TENISOMETER

The SWCC for a soil is defined as the relationship between water content (soil wetness) and matric suction for the soil. Degree of saturation (Sr), gravimetric water content (w) or volumetric water content (Θ), are all related by the equation,

$$\theta = \frac{V_W}{V} = \frac{w.G_s}{1+e} = \frac{Sr.e}{1+e} \quad (7)$$

An idealized SWCC is presented in Fig. 16.

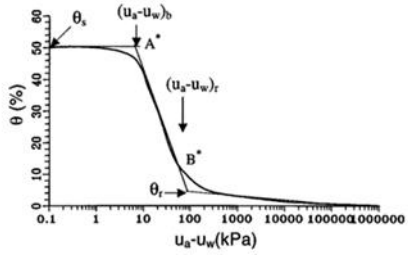

Fig. 16 Soil Water Characteristic curve

Continuous measurement method can be used to determine SWCC. Sample is gradually wetted and dried and their suctions were monitored continuously. The sample's weight was also continuously measured.

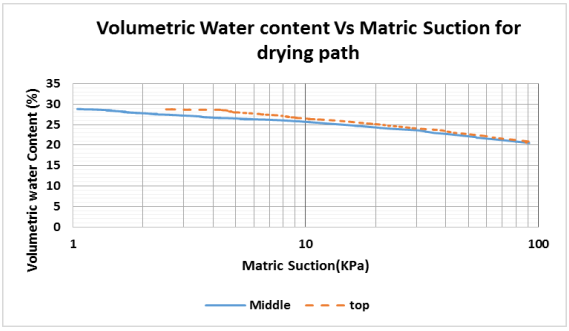

Fig.9 SWCC for drying path

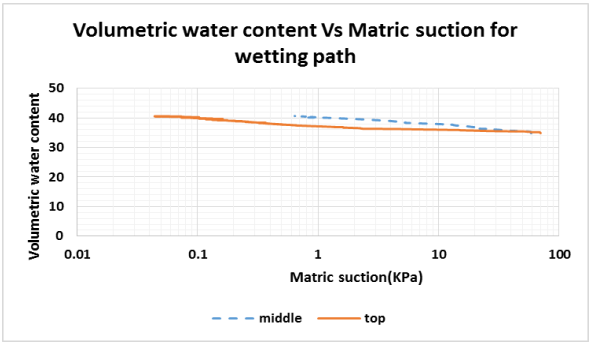

Fig. 11 SWCC for wetting path

7 CONCLUSION

Failures in natural slopes and embankments are frequently seen in the rainy seasons. This is due to the loss of matric suction or development of perched water tables due to prolonged rainfall and infiltration. SWCC, Permeability function and unsaturated shear strength parameters are the necessary input parameters in the understanding of these failures. With the establishment of these parameters for residual soils in Sri Lanka, the process of rainfall infiltration and loss of matric suction can be modeled. Slope stability analyses can then be conducted by incorporating these changes in the slopes and rainfall values. KU-Tenisometers can be used to monitor the changes in the pore pressures in the field as well. Field data can be compared with predicted changes from the modelling process and the model can be calibrated

6 REFERENCES

Fredlund, D. G. & Rahardjo, H., 1993. *Soil mechanics for unsaturated soils.* New York, Wiley: s.n.

Jotisankasa, A. & Mairaing, W., 2010. Suction-monitored direct shear testing of residual soils from landslide-prone areas. *Journal of Geotechnical and Geoenvironmental Engineering, ASCE,* Volume 136, p. 3.

Jotisankasa, A. et al., 2010. *Unsaturated soil testing for slope studies.* Chiangmai, Thailand., Proc. International conference on Slope, Thailand.

Sujeevan, V. & Kulathilaka, S., 2011. Rainfall Infiltration Analysis in Unsaturated Residual Soil slopes. *Journal of the Sri Lankan Geotechnical Society, Sri Lanka.*

Vasanthan, N 2016, "*Establishment of Fundemental Characteristics of Unsaturated Sri Lankan Residual Soils*", M.Eng thesis, University of Moratuwa, Sri Lanka

Use of Stone Columns in Very Soft Clays

M. H. M. Harshani
Department of Civil Engineering, University of Moratuwa, Sri Lanka

ABSTRACT: Stone column reinforced ground can be considered as a composite ground which has improved bearing capacity and stiffness compared to untreated ground with very soft clay. Significant settlement reduction while minimizing shear failures during construction are achieved by improving subsoil using this technique. In the research, a study was done on the effectiveness of geosynthetic encased stone columns (GESCs) as a solution to improve a thick layer of very soft clay, avoiding bulging of columns due to lack of confinement from surrounding soil. The performance of GESCs is analyzed using finite element method based software Plaxis 3D. With the results of the numerical analysis the effectiveness of the technique in settlement reduction, improvement in slope stability and acceleration in pore water pressure dissipation is confirmed.

1 INTRODUCTION

1.1 Stone Columns in General

Stone column technique is a widely used ground improvement method which has proven success in construction field. The technique is very useful at present due to its ability to provide workable solutions in infrastructure development through sites underlain by thick layers of soft clay. Stone column (SC) technique is accepted as feasible, environmental friendly, time and cost saving method which possesses many advantages. It reduces both total settlements and post construction settlements significantly and also avoids shear failures of embankment on soft soil during construction by reinforcing and load transfer. Accelerating the rate of consolidation is another advantage which is due to drainage paths created by granular columns to dissipate excess pore water pressure developed highly compressible soft soil. Further it contributes to mitigate liquefaction potential of sand in earthquake-prone areas. This technique is normally used when stabilizing large area loads like road embankments than concentrated loads. Stone column technique is specially adopted when comparably high road embankments are to be supported on the very thick layer of soft soil.

The uniform grid pattern (square or triangular) adopted for installing stone columns reduces the possibility of occurrence of differential settlements as soil properties are homogeneously varied in the treated ground. According to classifications, stone columns belong to granular flexible column category. Normally granular columns like stone columns are installed using vibro methods including replacement and displacement method or cased borehole method.

When considering load transfer mechanisms in stone columns, apart from lateral bulging, the shear stress developed along the soil/stone column interface and end bearing at tip of the column will additionally transfer loads to the surrounding soil. Further it is found that area replacement ratios of 25% or greater is needed for considerable improvement in bearing capacity *(McCabe 2007)*.

1.2 Geosynthetic Encased Stone Columns(GESCs)

Installation of stone columns in very soft clays is not generally recommended due to very limited confinement resistance offered by the surrounding soil due to its low undrained shear strength. This problem has been overcome by having geotextile encasement around the column preventing squeezing out of column material in to the soft soil. Basically bulging failures of columns can be minimized by increasing the bearing capacity by encasing them. The encasement having appropriate axial stiffness is adopted to improve performance of these columns. In addition to the bulging failures, upper portion of the column may subject to crushing failure in weak soft soils *(Chen, 2015)*. Geosynthetic encased columns could possibly fail from bursting of the geosynthetic encasement *(Han, 2014)*.

In the research, one of the objectives is to identify solutions to overcome bulging failures of stone columns constructed in very soft clays. Effectiveness of stone columns in settlement reduction and stability of slopes supported on ground treated by stone columns can be evaluated by finite element analysis. Numerical method such as finite element method was used in the research as it eliminates most of the limitations of other analysis methods.

2 METHODALOGY

2.1 Finite Element Analysis

2.1.1 Modeling Method

Widely used commercial finite element software, PLAXIS 3D was used in the study. It is capable of simulating the construction sequence of GESC. In the research coupled consolidation analysis are done adopting drained soil parameters as it simulates the actual construction process in a reasonable manner. Apart from the 3D model, unit cell idealization and 2D plain strain model are two approaches that many researchers have used. In axisymmetric unit cell model, dimensions in rectangular grid are converted to equivalent diameter of unit cell and the slenderness may result in numerical errors. The 2D

plain strain model is not capable of conversion of effect of axial stiffness of geotextile encasement to a 2D formulation. It models the whole domain of embankment instead of a single column (as a unit cell). Further, there are possibilities of errors occurring due to 2D conversion of a real 3D problem. As such, after initially trying out axisymmetric idealization it was decided to adopt 3D modeling in the study.

2.1.2 3D Finite Element Model

Considering the symmetry, one half of embankment and only the centerline of row of columns is modeled with 0.75m longitudinal length of embankment to avoid repetition of structures and to reduce the complexity of the problem along with running time of program (***Figure 1***). The embankment loading is taken as the loading configuration of the problem as stone column technique is mostly used in practice with such spread loading applications (***Figure 2***).

The vertical boundaries are fixed in horizontal direction and movement is allowed in vertical direction and full fixity is adopted at the base. Assuming singly drained condition, only Z_{max} is set to open in ground water flow condition. Stone columns are modeled as volumetric elements and encasement is modeled as a geogrid element.

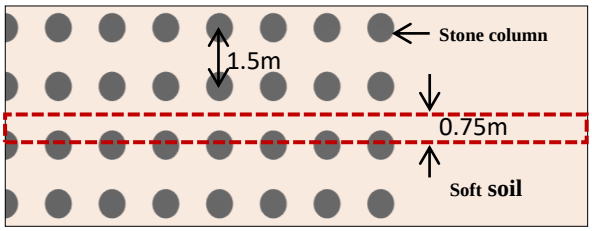

Figure 1: Representative unit considered in analysis (plan view)

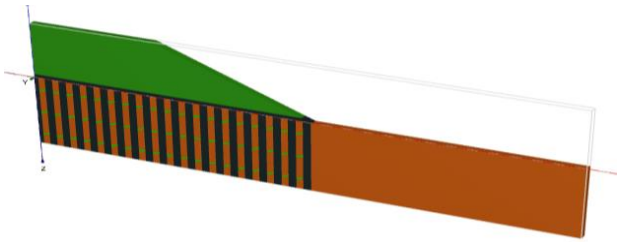

Figure 2: 3D model of geosynthetic encased stone column reinforced ground

2.1.3 Soil Properties Used in Modeling

Material properties and parameters used to represent the very soft clay, embankment fill and stone column material are presented in ***Table 1***. Mohr coulomb failure criterion is used as material model and drained parameters are adopted. Axial stiffness of geotextile is taken as 2000kN/m with isotropic behavior. The very soft clay is represented by applying low E value (400kN/m^2) as compared to stone column material.

Table 1 : Soil properties

Material properties	SC material	Emb. fill	Soft soil
γ_{unsat}(kN/m^3)	20	18	13
γ_{sat}(kN/m^3)	20	20	15
k_x ,k_y(m/day)	1	0.05	2×10^{-3}
k_z(m/day)	1	0.05	1×10^{-3}
E_{ref} (kN/m^2)	50000	20000	400
ν(nu)	0.2	0.3	0.35
C_{ref}(kN/m^2)	0.1	10	0.1 (D)
ϕ (°)	36	30	26 (D)
Ψ (°)	6	0	0

2.2 Simulation Process

Ground water table is taken to be at the existing ground, just below the drainage layer representing the worst case. Embankment construction is done mainly in two stages, namely; construction of 0.5m thick drainage layer and construction of embankment fill at a construction rate of 0.5m/week.

2.3 Different Cases Considered in Analysis

Parametric analysis - In the research embankment height and friction angle of stone column material are varied to cover the range of parameters encountered in practice.

Comparative analysis – The effectiveness of encased stone column is compared with untreated ground and stone columns without any encasement (Refer ***Table 2*** and ***Table 3***).

Table 2: Different models used

Model	Model description
M1	Untreated ground
M2	SC without geotextile encasement
M3	SC with geotextile encasement

Table 3: Details of the model

Soft clay	Thickness – 10m
Drainage layer	Thickness- 0.5m Used stone column material
Embankment fill	Height –6m, 8m, 10m Construction rate- 0.5m/week Three stages with drainage layer
Geotextile	Axial stiffness (EA) =2000 kN/m
Stone column	Length = 10m , Spacing = 1.5m Diameter =0.8m Area replacement ratio(A_r) = 22% Material–crushed stone, ϕ°-36˚,42˚

3 RESULTS AND DISCUSSIONS

With the simulation of the progress of the construction of the embankment at a rate of 0.5m/week using PLAXIS 3D, the variation of the settlement over the width and the variation of the safety margin with the increase of embankment height was studied.

3.1 Comparison of settlement reduction

Variation of maximum settlement as the construction progressed is presented in ***Figure 3***. There is considerable reduction of settlement (in the range of 13-26%) with the use of encased stone columns. The reduction is greater when the friction angle of stone column material is higher. With the encasement of stone columns there is a further reduction in settlement but the reduction was less significant.

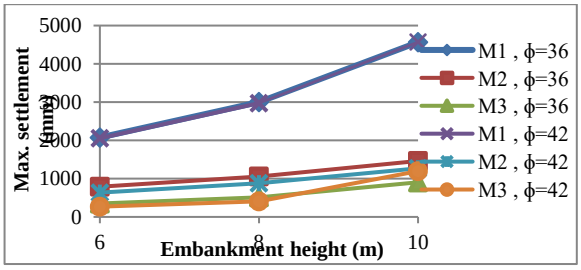

Figure 3: Maximum settlement at top of the embankment

The settlements are very high in the order of 4m when the stone columns are not used (***Figure 4***) in construction of embankments up to height of 10m. With the usage of stone columns the settlements are reduced below the order of 1m.

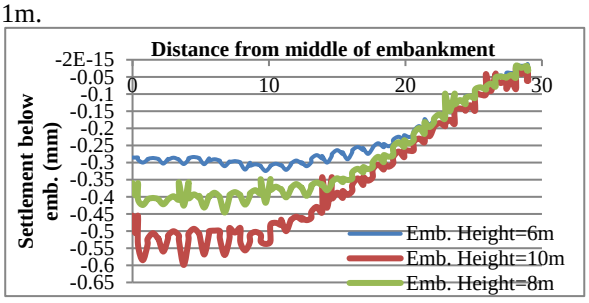

Figure 4: Settlement variation just below the embankment

The variation of settlement over the width of the embankment is plotted to the case of model M3 for the angle of internal friction of stone column material, 36˚ (refer ***Figure 4***). It shows that the settlement close to the center of the embankment was found to be the maximum and it increased with the height of embankment.

3.2 FOS Variation (Stability) Between Models

PLAXIS program gives the factor of safety indirectly using phi/c reduction technique. Here shear strength parameters are reduced by same rate, increasing the rate until the displacement increased rapidly. The rate at that time is taken as the factor of safety.

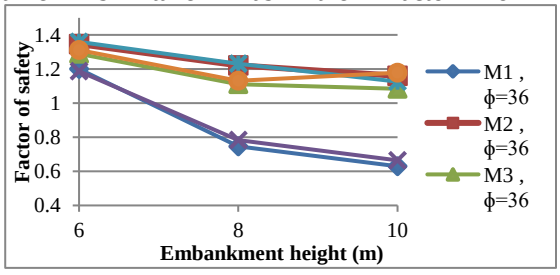

Figure 5: Factor of safety variation after construction of embankment

The variation of FOS of the embankment with increasing height is presented in ***Figure 5***. It shows that the FOS reduces drastically with the increase of embankment height when stone columns are not used. FOS values are less than 1.0 when the embankment height exceeds 6m in untreated ground. When stone columns are present, the FOS was maintained above 1.0 for the embankment heights up to 10m and the reduction of FOS with embankment height is not drastic (***Figure 5***).

3.3 Effect of Stress Concentration

The phenomenon called stress concentration implies that great portion of load is taken by the stone column due to the stiffness difference between soft soil and column material. Stress concentration ratio (n) is the ratio of stress on the column to that of the soft soil. Stress concentration effect is automatically computed in the PLAXIS simulation process.

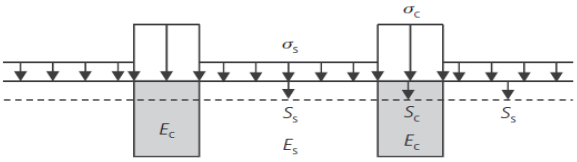

Figure 6: Representation of stress concentration phenomena

In conventional designs it has to be assumed and an empirical equation (***Eqn. (1)***) used in general is: $\boldsymbol{n = a + b(E_c/E_s)}$ where a, b is empirical parameters and E_c and E_s are modulus of elasticity of stone column material and soft soil respectively. The variation of vertical stress at the stone columns and in the soft clay material for the 6m high embankment and 10m high embankment are illustrated in ***Figure 7*** and ***Figure 8*** respectively.

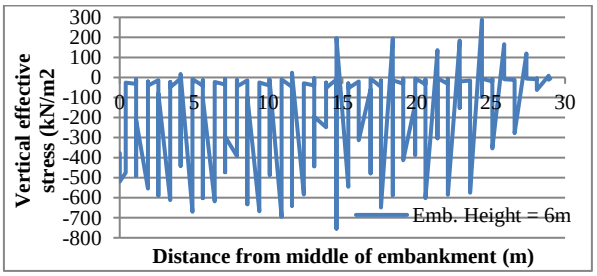

Figure 7: Stress concentration for 6m high embankment

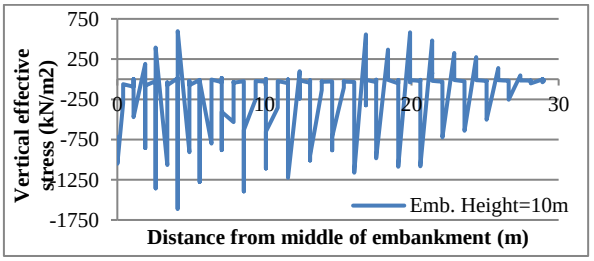

Figure 8: Stress concentration for 10m high embankment

According to empirical ***Eqn. (1)***, the n value is 28 which did not change with the embankment height. In the

analysis done with PLAXIS the average stress concentration factor calculated is about 18 and 16 for the embankment heights of 6m and 10m respectively which varies with embankment height.

3.4 Plastic Points

With the progressive construction of the embankment without stone columns the FOS reduced to values less than 1.0. With the use of stone columns FOS value remained above unity (1.0). As FOS approaches unity, more elements should approach failure. As such there should be less number of plastic points. The unusual pattern of large number of plastic points even when the stone columns are used (***Figure 9***) had to be attributed to numerical errors at the front interface of stone column/soft clay due to large difference of modulus of elasticity(E) between soft soil and SC material. Later when a sensitivity analysis is conducted by reducing the gap between E value of soft soil and SC material, then the number of plastic points reduced.

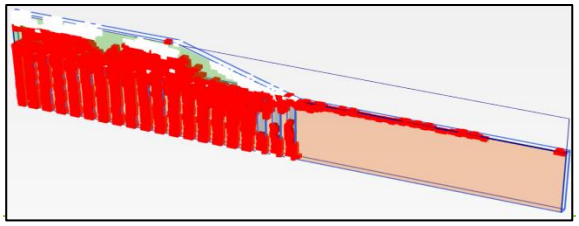

Figure 9: Plastic point distribution (indicated in red squares) at the interface of stone column /soft soil

3.5 Porewater Pressure Distribution

Porewater pressure dissipation is accelerated in stone column reinforced ground due to the high permeability of material forming columns. ***Figure 10*** presents a comparison of excess pwp after construction of embankment to the height of 6m between M1, M2 and M3 models. These results show that when the stone columns are present, the excess pore water pressure is completely dissipated.

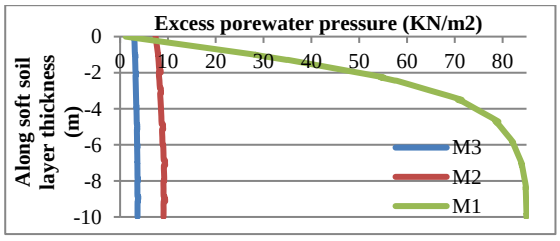

Figure 10: Excess pwp variation along vertical length of soft soil

3.6 Deformed Shapes and Failure Mechanisms

Deformation patterns and failure modes of stone column reinforced ground are needed to be identified to ensure safe construction. Lateral spreading and circular failure are the common types of failure with the application of embankment loading on soft soil.

The effectiveness of stone columns in restraining deformation is illustrated in ***Figure 11*** by comparison of the case of the construction of an embankment of height, 6m. The settlements and lateral deformations are very high (M1-plotted to true scale) when there are no stone columns. When there are stone columns without encasement, deformations (M2-scaled up 5 times) have reduced. There is a further reduction of deformation in encased stone columns (M3).

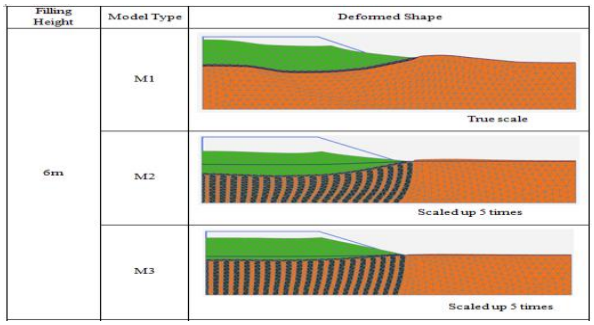

Figure 11: Deformed mesh for 6m high embankment

4 CONCLUSIONS

Finite element analysis is carried out using PLAXIS 3D software to study the performance of encased stone columns. It can be concluded that comparing to untreated ground, stone column reinforced ground displayed significant settlement reduction; hence it has proved as effective method in reducing settlements. Also factor of safety did not decrease to values lower than 1 as the embankment height increased.

There were further reductions (although not very significant) in settlements and increases in factor of safety when the stone columns were encased. The stone columns caused a reduction in lateral deformations with the construction of embankment. The encasing of stone columns caused a further reduction in lateral deformations.

Furthermore, the finite element results illustrated that significant reduction of excess pwp in reinforced ground due to increased rate of consolidation comparing to untreated ground. The stress concentration factor appears to be changing with the embankment height in contrast to the assumption made in the empirical formulae used in conventional analysis.

ACKNOWLEDGEMENT

The authors would like to express their gratitude to Dr. Nalin de Silva for his valuable guidance in the research.

5 REFERENCES

Chen, J.-F. L.-Y.-F.-Z. (2015). Failure mechanism of geosynthetic-encased stone columns in soft soils under embankment. *Geotextiles and Geommbranes*, 1-8.

Han, J. (2014). Recent research and development of ground column technologies. *Institution of Civil Engineers.* ICE.

McCabe, B. A. (2007). Ground improvement using the vibro-stone column technique. *Joint meeting of Engineers Ireland West Region and the Geotechnical Society of Ireland.* NUI Galwa

Evaluation of Pullout Resistance of Grouted Soil-Nails

D.W. Jayasekara
Department of Civil and Environmental Engineering, University of Ruhuna, Sri Lanka

ABSTRACT: Soil-nailing is one of the most commonly adopted techniques to stabilize the cut slopes especially in the congested areas. However, geotechnical engineers use different methods for soil-nailing design as there is no any accepted design methods for soil-nailing. Based on the field pullout test results, many researchers found that measured pullout force in the field is much higher than the designed pullout force. As such, current method of soil-nailing practice has tended towards the safe rather than the most economical solution as soil-nail interaction is more complex. Therefore, in this research study, the behaviour of grouted soil-nails was investigated during pullout by varying overburden pressure with the help of a laboratory setup. The results were verified numerically. In addition, earth pressure transducers were installed in the laboratory model to observe the vertical stress variation during pullout test. It was revealed that the dilatancy effect played a significant role during pullout.

1 INTRODUCTION

Many failures have been reported recently in Sri Lanka due to instability of slopes and retaining structures. In order to stabilize those slopes, soil-nailing technique has been successfully applied in the field due to its attractive features such as low cost, low construction period, less working area and minimum environmental impact (Watkins and Powell, 1992).

Pullout resistance is the most critical parameter in soil-nailing that should be estimated precisely during designing. However it is difficult to estimate this parameter accurately due to uncertainties related to soil-nail pullout interaction. Generally, theoretical pullout force (f_theoretical) values are calculated based on the equation 1,

$$f_{\text{theoretical}} = \pi D l (c' + \sigma' \tan \varphi') \quad (1)$$

Where D is the soil-nail diameter, l is the soil-nail length,c',φ' are the effective shear strength parameters of surrounding soil and σ' is the effective vertical stress.

Many researchers (Pradhan et al., 2006; Milligan and Tei, 1998; Junaideen et al., 2004; Zhang et al., 2009) have conducted field and laboratory pullout tests to investigate the behaviour of soil-nails. Junaideen et al., 2004 prepared a large laboratory setup to study the soil-nail interaction in loose fill materials with a large box (2 m long × 1.6 m wide × 1. 4 m high) to put-up soil samples and soil-nails, two portal frames (2.4 m high ×2.4 m wide) to apply vertical pressure at the top of the box and a pulling device to pull the nails at a constant rate. In addition, six Earth Pressure Transducers (EPT) were installed in soil fill, 50mm above the soil-nails to measure the vertical pressures generated. The test results proved that the normal stress acting above the soil-nail changes during pullout due to dilatancy effect. Furthermore Linear Variable Displacement Transducers (LVDT) were installed by Gurpersaud et al., 2010 to measure applied force and displacement. The data was recorded using a Data Acquisition System (DAS). Although many laboratory and field tests are conducted, the behaviour of soil-nails during pullout is not fully understood. Therefore the pullout resistance measured in the field is much higher than the value expected from the design. So this research study was conducted to investigate the behaviour of grouted soil-nails during pullout by varying overburden pressure. In addition, three EPT were installed, 50 mm above the soil-nail to investigate the vertical stress variation during pullout. The results were verified numerically.

2 METHODOLOGY

2.1 *Material selection and determination of basic soil properties*

Soil was selected from a Soil-nailing site at Halloluwa-Katugastota road in Kandy in Sri Lanka and basic soil properties were determined in the laboratory and depicted in Table 1. Soil type was classified as well graded sand and gravelly sand with little or no fines (SW) according to Unified Soil Classification System (USCS). The effective friction angle and effective cohesion are 43° and 25 kPa respectively.

25-32 mm diameter soil-nails are used in field condition. But compared to mould size, it is impossible to use such kind of large diameters for model

analysis. In addition, Meethananda et al. revealed that there is a less effect on increase of pullout force compared with increase of nail diameter. Furthermore, it is concluded that there is a significant increase of pullout force of ribbed bars compared to plain bars. Therefore, a 10 mm diameter Tore steel ribbed reinforcement bar was used for the laboratory model analysis.

Table 1. Physical properties of soil

Property	Value
Liquid limit (%)	33
Plastic limit (%)	28
Plasticity index (%)	5
Optimum moisture content (%)	13.5
Maximum dry unit weight (kN/m^2)	18.6
Specific gravity	2.38
Coefficient of uniformity	6.25

2.2 *Test box preparation*

A steel mould with internal dimensions of 610 mm×480 mm × 600 mm was used as the test box. The soil obtained from soil-nailing site at Kandy was completely compacted in the test box at 95 % of the optimum moisture content in 50 mm layers. After compaction of soil up to 300 mm height, soil-nail was installed and compaction was continued to fill the text box. Three Earth Pressure Transducers (EPT) were placed 50 mm above head, middle and tail of nail during compaction. A pullout jack was fixed to the nail head in order to pull the nail outwards.

2.3 *Arrangement for drilling and grouting*

The hole for installation of nail was manually drilled horizontally by using a hand auger of 50 mm diameter. The soil-nail was placed in the middle of the drilled hole by using centralizers and then hole was grouted by applying pressure.
For the application of the grout pressure another model was prepared. Here a grout tank of 3L was used having 3 openings for pouring of grout, application of air pressure and flowing of pressurized grout. Here the air pressure was applied by using a compressor and the compressor gauge was used to measure the grout pressure. The grout pressure used was 100 kPa and was a constant parameter for this test series.

2.4 *Instrumentation*

Overburden pressure was applied to the test box by using two hydraulic jacks fixed to a portal frame and monitored by a load cell. A dial gauge was fixed to the nail head to monitor the horizontal displacement of the soil-nail during pullout. A pullout jack was used to pullout the soil-nail and a pressure gauge connected to the jack was used to record the hydraulic pressure required in soil-nail pullout test. Before proceed the test, a calibration test was conducted to identify the force corresponds to the recorded fluid pressure. In addition, a dial gauge was attached to the free end of soil-nail to measure the horizontal displacementduring pullout test and another two dial gauges were attached at the top of test box (on steel plate) directly above the soil-nail head and tail to measure vertical displacement of soil during pullout. Fig.1 shows the prepared laboratory model setup.

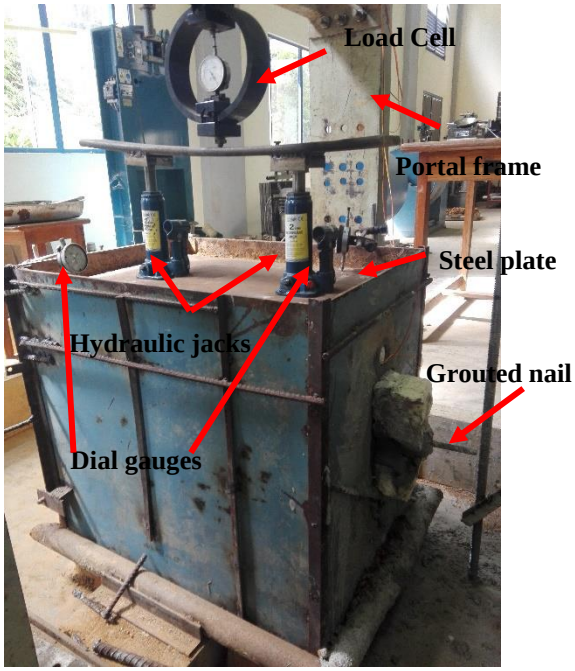

Fig. 1 Laboratory model setup

2.5 *Testing procedure*

The pullout test was conducted in a displacement controlled manner with the help of pullout jack after 7 days of grouting. Pullout tests were conducted by changing surcharge as 20 kPa, 40 kPa, 60 kPa and 80 kPa.

2.6 *Numerical analysis*

The laboratory model was drawn in PLAXIS 2D software and the boundary conditions were applied. Standard fixities option was used, so that a full fixity at base of the geometry and roller conditions at the vertical sides were generated. Plate was used to model the soil-nail and an interface was introduced between soil and nail. An overburden pressure was applied at the top of the mould as shown in Fig. 02.

Materials were assigned into soil, plate and interface according to the properties used in the laboratory test. After assigning materials, a mesh was generated and initial condition was defined in

the model (ground water condition). The model was analyzed using Mohr-Coulomb failure criteria.

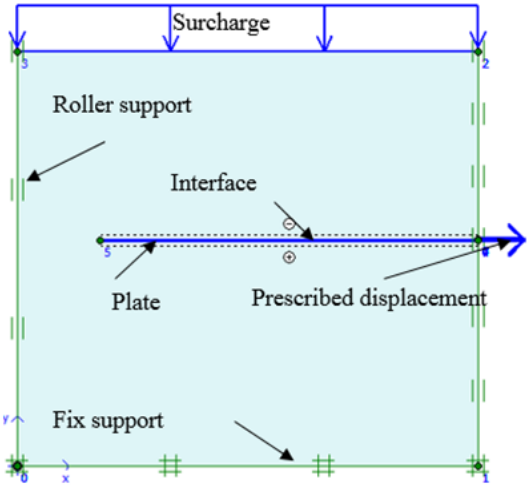

Fig. 2Model drawn in PLAXIS 2D software

A prescribed horizontal displacement was given to the free end of the nail and thereby the nail behaviour was obtained by varying the horizontal displacement of the nail. In numerical model, laboratory condition was simulated in staged construction mode. The phrases used for the staged construction mode are summarized as follows.

- Initial phase: Only the soil fill in the model was activated and all the structures and external forces were inactivated. Normally this condition is given by the software in default.
- Phase 1: Plate and interface were activated.
- Phase 2: Overburden pressure was activated.
- Phase 3: Prescribed displacement was activated (the displacement that gives highest pullout in laboratory experiment was used as the value for prescribed displacement).

The overburden pressure was changed from 20 kPa to 80 kPa and model was run to obtain the maximum shear stress at soil-nail interface in each case.

3 RESULTS AND CONCLUSION

Fig. 03 shows the variation of pullout force with overburden pressure resulted from laboratory tests. It can be seen that the pullout force increases up to a peak value and decreases with soil-nail displacement and eventually reaches to a constant value. Therefore peak pullout force can be considered as the maximum pullout force mobilized at the soil and grouted nail interface.

Fig. 04 shows the vertical stress distribution near nail head and tail for 40 kPa surcharge during pullout test. According to the pressure sensor results, the vertical stress near nail head is higher than nail tail and vertical stress variation can be seen only during the pullout test.

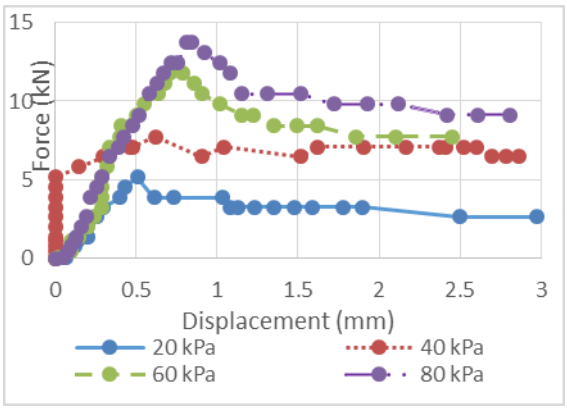

Fig. 3Pullout force variation with surcharges

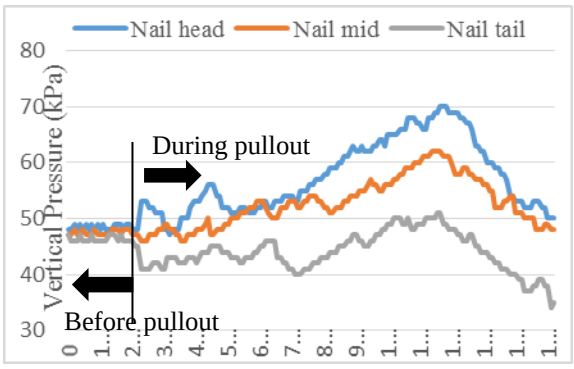

Fig. 4Indication of vertical stress on nail before and during pullout

Fig. 05 proves that the tendency to move soil near nail head is higher than nail tail by using dial gauge readings.So it can be concluded that the dilatancy effect near nail head is higher than nail tail. As a result, the vertical stress near nail head would be higher than nail tail.

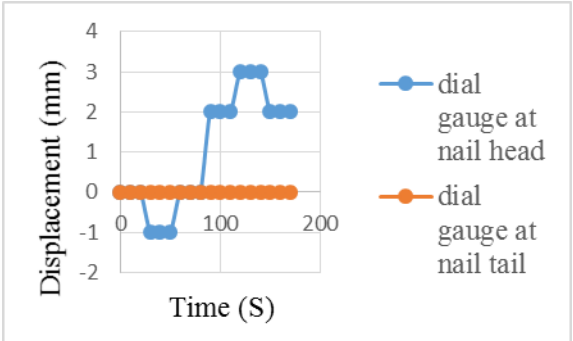

Fig. 5Dial gauge readings above nail head and tail

In numerical analysis, the shear stress distribution along soil-grout interface was considered as it is the failure plane observed from laboratory mod-

el. The highest shear stress is generated near nail head due to higher dilation effect. Fig. 6 shows the variation of theoretical, numerical and experimental pullout forces with surcharges. Theoretical pullout values were calculated using Equation 1. The laboratory pullout force is 1.68-2.46 times higher than theoretical pullout force. So it is clear that there is an overdesign in soil-nailing.In addition, it is clear that there is a good relationship between laboratory and numerical pullout forces.

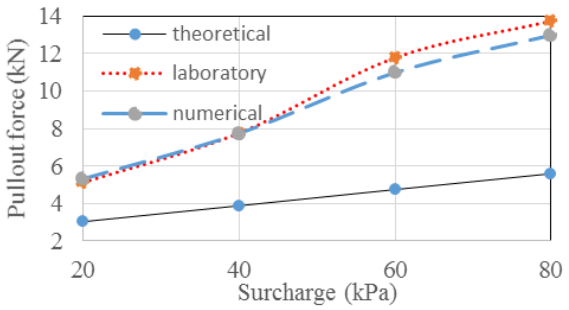

Fig. 6Variation of pullout forces with surcharge

Fig. 7 shows the vertical stress variation during pullout using numerical analysis for 40 kN/m^2 surcharge. So, it is clear that the highest vertical stress was occurred at the nail head and least vertical stress was occurred at nail tail. The reason behind this would be the dilation effect on pullout force. Because of volume increase and decrease due to dilation, the soil particles may be loose or tight. So the normal stress act on soil-nail may change during shearing.

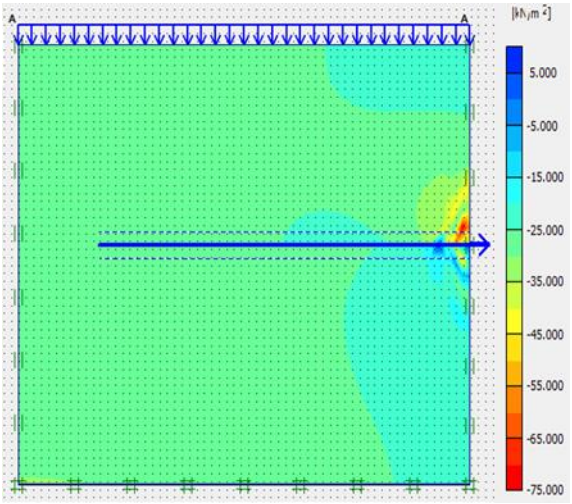

Fig. 7Vertical stress variation during pullout for 40kPa surcharge

It is clear that there is an overdesign in soil nailing. One reason for this may be dilatancy as it plays a significant role during pullout. So analytical models including dilatancy effect should be used for soil nailing designing.

ACKNOWLEDGMENTS

The writers would like to acknowledge the support given by Department of Civil and Environmental Engineering, the University of Ruhuna.

REFERENCES

Gurpersaud, N., (2000)., 'The influence of matric suction on the pullout capacity ofgrouted soil nails', MSc.thesis, Department of Civil and Environmental Engineering,Carleton University.

Junaideen, S. M., Tham, L. G., Law, K. T., Lee, C. F. and Yue, Z. Q., (2004)., 'Laboratory study of soil nail interaction in loose, completely decomposed granite', Canadian Geotechnical Journal, 274-286.

Meetananda, D. C. A., Premarathne., B. D. H. and Priyantha, H. M. S., (2011)., 'The use of soil nailingtechnique in stabilizing slopes', Final year research project, Dept. of Civil Engineering, University ofMoratuwa.

Milligan, G. W. and Tei, K., (1998)., 'The pullout resistance of model soil nails', Soils and Foundations 38(2), 179-190.

Pradhan, B., Tham, L. G., Yue, Z. Q., Junaideen, S. M. and Lee, C. F., (2006)., 'Soil–nail pullout interaction in loose fill materials, International Journal of Geomechanics, July-August,238-247.

Watkins, A. T. and Powell, G. E., (1992)., 'Soil nailing to existing slopes as landslip preventive works', Hong Kong Eng., 20, March, 20–27.

Zhang,L.L, Zhang, L.M. and Tang, W.H.,(2009)., 'Uncertainties of field pullout resistance of soils', Journal of Geotechnical and Geoenvironmental Engineering,135(7),966-972.

Effect of Low Calcium Fly Ash (ASTM class F) on Stabilization Behaviour of Expansive Soil

S.M.C.U. Senanayake, T.B.C.H. Dissanayake
Department of Civil Engineering, University of Peradeniya, Sri Lanka

ABSTRACT: Expansive soil experiences swelling with the addition of water and then shrink after the removal of water. These alternate wetting and drying impose lot of problems to the structures built on expansive soils. Ground improvement techniques for expansive soil include chemical and mechanical method of soil stabilization. In this paper, chemical stabilization has been used as a ground improvement technique. Testing such as compaction, unconfined compressive strength (UCS) and swell pressure were conducted for expansive soil stabilized with ASTM Class F fly ash as a chemical stabilizer at 8%, 16% and 24% of total weight. Based on the outcome of this study, it was noticed that maximum dry density (MDD) increases up to 16% and then decreases beyond that. Effect of fly ash on variation of UCS value was observed with three different curing periods (7, 28 and 45 days) as well as three different percentages of fly ash (8%, 16%, 24%). UCS values increase up to 16% and then they decrease with any further addition of fly ash. Further, increment of curing period helps to increase the UCS value for a given percentage of fly ash mixture. Reduction of swell pressure was observed with addition of fly ash. On the whole, fly ash can be successfully used as soil stabilized to improve the geotechnical engineering properties of expansive soil.

1 INTRODUCTION

The Expansive soils subjected to swelling and shrinkage with the absorbing or evaporation of water and therefore, it involves high range of change in volume. Kaolinite, Montmorillonite, illite components in the expansive soil are the major components which undergoes alternative swelling and shrinkage behavior (Hansgeorg, 2006). Low bearing capacity, high settlement, less shear strength and heaving are major problems encountered when construction works are going on expansive soils. Soil stabilization techniques are used to mitigate unfavorable conditions associated with expansive soils and these techniques are categorized into mechanical and chemical methods. Mechanical methods consists soil replacement technique, vibroflotation etc. while chemical methods stabilize soil by adding different chemical compounds such as lime, fly ash, cement etc.(Somaiya et al,2013).

Fly ash is a solid waste which is generated in coal power plants after the combustion of coal. They cause for several environmental hazards if these solid waste is not properly managed in an effective manner. In Sri Lanka, Norachcholai coal power plant generates about 75000 tons of fly ash annually and some of them are used in cement manufacturing process while keeping remaining fly ash causing environmental pollutant. So, it is a sustainable solution for utilization of fly ash in stabilizing soil. Fly ash can be classified as high calcium fly ash (ASTM class C) and low calcium fly ash (ASTM class F) based on the standards of American Society for Testing and Materials. In this study focuses on chemical stabilization of expansive soil by varying percentage of fly ash by weight as chemical admixture. There are many previous studies by Fusheng et.al ,Estabragh and Pereshkafti, Somaiya et.al,Deng et.al focusing on stabilization of soft soil using different chemical stabilizers by various researchers are summarized below.

Fusheng et.al (2008): studied about the high plasticity silty clay stabilized with fly ash and lime at varying percentages. Atterberg limit test, Free swell test, Compaction tests and UCS tests were performed during the experimental study. Main conclusions of their study were liquid limit decreases with addition of fly ash and lime, MDD and OMC decreases with addition of additives. Finally UCS value of tested samples were increased with ash addition up to an optimum and beyond the it decreases with fly ash and lime addition due to the enhanced rate of pozzolanic reaction and flocculation in the stabilized soil mix.

Estabragh and Pereshkafti (2012): A similar comparative study was carried out on high plasticity clay using lime, cement and coal ash as chemical stabilizers. They studied the effect of cyclic wetting and drying as well as compaction characteristics investigated. Main conclusions of this study were liquid limit and plasticity index can be increased with coal ash and cement content, MDD and swelling can be reduced up on addition of additives. Lime and cement showed equilibrium state after 2nd cycle and 4th cycle respectively. Somaiya et. al (2013) :Expansive soil causes for major prob-

lems such as heaving when constructions are going on soft ground. In this study, expansive clay stabilized using fly ash as chemical stabilizer. Variation of Atterberg limits, variation of MDD and OMC, variation of UCS with addition of fly ash investigated during this study. Main conclusions were liquid limit and plastic limit reduces with fly ash addition. MDD value of the stabilized soil sample initially decreased to a minimum value and then increased any further ash addition. UCS values of the tested samples initially increases up to an optimum value and then it reduces.

Deng et al (2007): Comparative study using sewage sludge ash and class F fly ash on low plasticity silty clay was done. Mainly pH value test and UCS test carried out during the experimental study. They revealed that, UCS values of soil sample stabilized with fly ash mixture is less than sludge ash treated soil samples due to the variation of chemical composition of fly ash and sludge ash. It is observed that fly ash treated soil samples have much higher pH than soil stabilized with sewage sludge ash. Finally, main conclusion is, fly ash can effectively be substituted by sewage sludge ash in soil stabilization. Laxmikant and Tripathi (2013): Ground granulated blast furnace slag (GBS) and fly ash used to stabilize high plasticity silty clay. Variation of California bearing capacity (CBR) and compaction characteristics studied and key findings of their study were CBR value of the mixture reduces with fly ash and GBS addition. Results indicate that MDD value increases with GBS content while keeping fly ash content constant in the mixture and OMC increases with fly ash and GBS simultaneously.

To date there are very limited studies focusing on the stabilization behaviour of ASTM Class F fly ash to improve expansive soil, and hence major aim of this research is to study the geotechnical engineering properties of expansive soil treated with fly ash.

2 MATERIALS AND METHODOLOGY

In this study, fly ash is used to stabilize expansive soil which is obtained from Nikkakatiya, Digana, Sri Lanka while fly ash were provided by Holcim Lanka Ltd, Colombo, Sri Lanka. Expansiveness of soil was determined by conducting free swell test. Test result illustrates that free swell ratio is 1.55 and soil is moderately expansive soil according to the classification by Holtz and Gibbs in1956.Gradation of natural soil is shown in Figure 1 and chemical composition of fly ash is shown in Table 1.

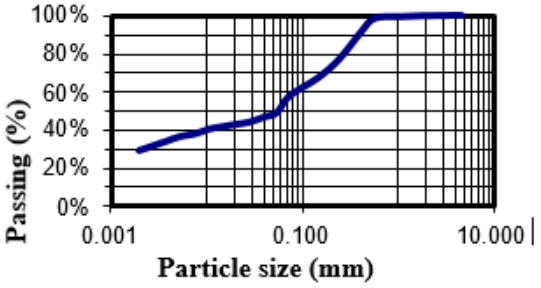

Fig 01.Particle size distribution of expansive soil

Table 01. Chemical composition of fly ash

Composition	Percentage by weight
SiO_2	52.03
Al_2O_3	32.31
Fe_2O_3	7.04
CaO	5.55
MgO	1.3
SO_3	0.07
K_2O	0.68
Na_2O	0.43

According to the gradation curve which is depicted in Figure 1, Soil can be classified as clayey soil sample. Soil samples for testing were prepared at 8%, 16%, 24% fly ash by weight with expansive soil after mixing thoroughly. To study the variation of MDD and OMC with fly ash content, A series of standard proctor compaction tests were done for each mix composition according to BS 1377, 1990 part 4. Variation of compressive strength of stabilized soil was observed by conducting a series of UCS tests according to BS 1377, 1990 part 7 and samples for this test were prepared at by compacting to MDD and OMC. Height of 76 mm and diameter of 38 mm samples were prepared while keeping aspect ratio is to 2. Samples were cured at ambient temperature (25 0C) for 7, 28, 45 days and tested for each curing period. For each data point three samples were tested to ensure reliability of test results. Swell pressure test was done according to BS 1377, 1990 part 5 and constant volume test was conducted to identify swelling behavior of stabilized soil samples.

3 RESULTS AND DISCUSSION

3.1 *Compaction Characteristics*

Standard proctor compaction test was done for natural expansive soil, fly ash treated soil samples to study the variation of MDD and OMC with addition of fly ash as chemical admixture. The variation of MDD is shown in Figure 2.

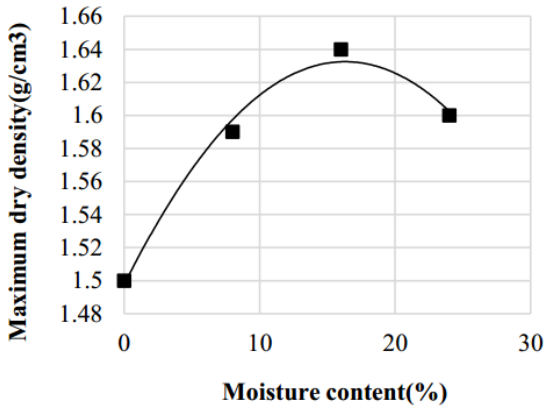

Fig 02. Variation of MDD with fly ash

Based on Figure 2, Initially MDD value is increased up to 16% ash content optimum value of a MDD can be achieved at 16% fly ash content and it is mainly due to flocculation with in soil sample caused by fly ash and well packing of soil particles also leading to the increment of MDD (Phanikumar ,2009). Beyond the optimum it decreases up to 24% fly ash content due to unreacted fly ash particles in the mix and lower specific gravity fly ash particles replacing soil particles causing resulting mix which is having a lower specific gravity.

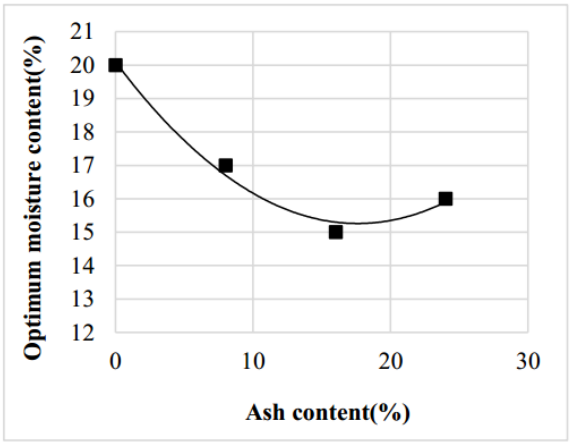

Fig. 03. Variation of OMC with fly ash

The variation of OMC with fly ash content is illustrated in Figure 3. Initially, OMC value decreases up to a 16% fly ash content and the cause for the reduction of moisture content up to a minimum value is mainly due to the cation exchange between additives. After OMC reaches to a minimum value, it starts to increase for any increase in OMC beyond the optimum. This kind of behavior can be seen because unreacted fly ash particles absorb more moisture and it leads to increment of OMC (Fusheng et al., 2008).

3.2 *Unconfined Compressive strength*

This test was performed to identify variation of UCS value with fly ash content and standard deviation of UCS values were 0-8%.Variation of UCS value with fly ash addition is shown in Figure 4.

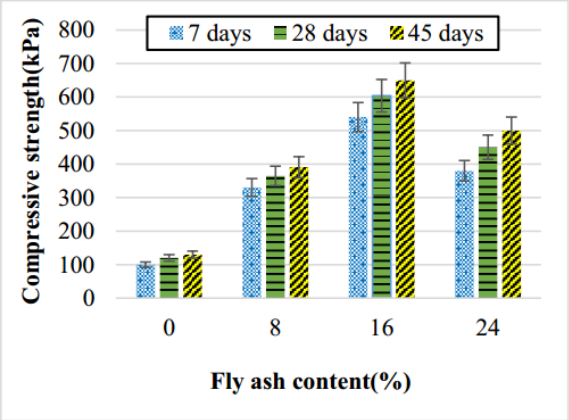

Fig. 04. Variation of UCS with fly ash

Based on Figure 4, UCS value initially increases up to 16% fly ash content and maximum increment is 540% for fly ash treated expansive soil sample at 45 days curing time. It is mainly due to the enhanced pozzolanic reaction and flocculation in the stabilized soil sample. Beyond the optimum, it reduces with ash content due to additional fly ash in the mix act as unbounded silt particles causing decrease in strength (Fusheng et al., 2008).

3.3 *Variation of swell pressure*

Series of swell pressure tests were conducted to investigate swelling behaviour of stabilized soil with fly ash as chemical admixture. Variation of swell pressure with ash content is shown in Figure 5.

According to figure 5, It can be seen that Swell pressure is decreased to 33 kPa from 113 kPa while adding more and more fly ash to expansive soil. Reduction of swell pressure is mainly caused by enhanced pozzolanic reaction and high surface area of fly ash particles. Formation of Calcium Silica Hydrate (CSH) and Calcium Alumina Hydrate (CAH) also helps to decrease in swell pressure (Fusheng et al., 2008).

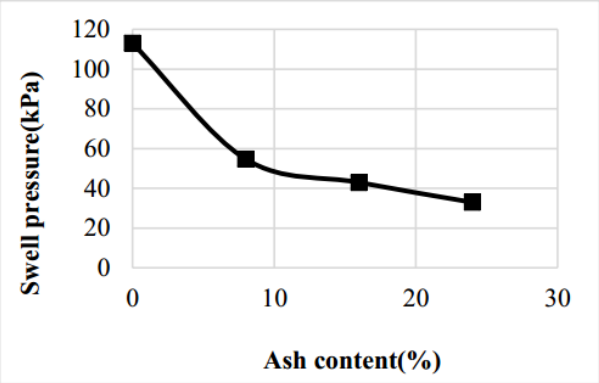

Fig. 05. Variation of swell pressure with fly ash

4 CONCLUSIONS

The following points provide important conclusions derived from this study on expansive soil,

• According to standard proctor compaction test results MDD value is initially increased to an optimum value and beyond that decreases. OMC value also decreases to a minimum value and after reaching to the minimum value it starts to increase. This shows that soil and additive mixture can be compacted with lower water content.
• UCS value of the treated soil is increased up to 16% and came to an optimum value. Highest UCS value can be seen at 45 days cured sample. Beyond the optimum UCS value starts to decrease. Reason for the increment of UCS is flocculation and enhanced pozzolanic reaction there of formation of cementitious materials such as CSH, CAH. Reduction of UCS caused by unreacted fly ash particles in the stabilized soil.
• Swell pressure is significantly reduced using fly ash as the chemical additive and it is due to the pozzolanic reaction and higher surface area of fly ash particles.

ACKNOWLEDGMENTS

The research was financially supported by University of Peradeniya and we are grateful to Holcim Lanka Ltd (INSEE cement) for giving fly ash.

5 REFERENCE

1) Bell F.G (1996), Lime stabilization of clay minerals and soils, Engineering Geology, vol 42:pp 223–237.
2) Deng-Frong L., Kae-LIong L., Huan-Lin L. ,(2007) Comparison between sludge ash and fly ash on the improvement in soft soil , ." Journal of the Air & Waste Management Association 57.1 : pp 59-64
3) Dujang B. Huat ,David G toll,Arun Prasad Handbook of tropical residual soils engineering edition 2012,CRC press: pp 139
4) Fusheng Z., Songyu L, Yanjun D., Kerui C. (2008), Behavior of expansive soil stabilized with FA, Natural hazards,vol 47(3), pp.509-523
5) Hansgeorg K, Berhane G, Excavations and Foundation in soft soils, Edition 2006, pp 11
6) Holtz, W. G. and Gibbs, H. J. (1956), Engineering properties of expansive clays,Transactions ASCE 121,pp 641-677
7) Laxmikant Y., Tripathi R.K. (2013), Stabilization of soft soil with granulated blast furnace slag (GBS) and fly ash (FA),." International Journal of Research in Engineering and Technology 2.2 (2013): 115-119.Journal of Pavement Engineering 14.4: pp 418-427
8) Phanikumar B. (2009), Effect of lime and FA on swell, consolidation, and shear strength characteristics of expansive clay. Comparative study, Geomechanics and Geoengineering international journal,vol 4.2 : pp 175-181
9) Priyadarshena T, Dissanayake R, Mendis P. (2015), Effect of nano silica, micro silica, FA and bottom ash on compressive strength of concrete, Journal of Civil Engineering and Architecture vol 9 : pp 1146-1152
10) Sivapullaiah, P.V. Prashanth, J.P. Sridharan A.(1996) ,effect of FA on the index properties of black cotton soil,soils and foundations vol. 36 (1996) no. 1 :pp 97-103
11) Somaiya P, Zala Y, Dangar R (2013); Stabilization of expansive soil using FA; Conference paper

Effect of temperature on mechanical behaviour of well cement: An Experimental study

A. Subaha and V. Aarany
Department of Civil Engineering, University of Peradeniya, Sri Lanka.

ABSTRACT: The construction of the wells for Carbon dioxide capture and storage deep underground has become a major challenge for the 21st century Engineers. Carbon dioxide sequestration deep underground has been identified as the best mitigation measure to reduce the concentration of carbon dioxide in the atmosphere, which expedites the global warming. Generally these underground well cementing's lose their integrity mainly due to the degradation caused by the aggressive curing temperature and salinity conditions prevailing in the earth's down-hole. In this phenomena, the effect of temperature is much higher than that of the salinity. Hence this research work focuses on the effect of temperature on the mechanical behavior of well cement under a given salinity. For this analysis the Sulphate resistant class G cement samples that were oven cured at varying curing temperatures of room temperature, 40 ^{0}C, 60 ^{0}C and 80 ^{0}C at a constant optimum salinity of 10% NaCl by weight of water were considered. To study the mechanical behavior of well cement, uniaxial compressive strength and Young's modulus were analyzed.

Key words: Carbon capture, Degradation, Salinity, Sequestration, Well cement, Introduction

1 INTRODUCTION

Global warming has been evolved as a massive problem which endangers lives on the earth. Out of the greenhouse gases causing the global warming, carbon dioxide (CO_2) plays a major role (Nasvi et al, 2012). Hence, it has become indispensable to reduce the concentration of carbon dioxide in the earth's atmosphere. As per the statistical data of World Meteorological Organization (WMO, 2015), it has been found that the concentration of CO_2 was about 400 part per million (ppm) in 2015.

Increasing usage of coal powered plants, petroleum usage and oil recovery seems to be the major ways of CO_2 emissions. Some of the mitigation measures to reduce the concentration of Carbon dioxide in the atmosphere are improving the energy conversion efficiency of fossil fuels, shifting energy production to low carbon sources and capturing and storing CO_2 deep underground (Barlet et al, 2009). Out of all these solutions capturing and injecting the CO_2 deep underground has been found to be the long term durable, economical, most favorable and efficient method (Sarmiento and Gruber, 2002; Gielen, 2003). It's very important to ensure the integrity of these sequestration underground reservoirs. The captured CO_2 is injected into the deep reservoirs and this kind of well is used for oil and gas reservoirs as well.

To ensure the integrity of the sequestration wells, zonal isolation in these wells is ensured by the steel casing and the primary cementing. Hence, the primary cement should be of better CO_2 resistance, high strength and resistance for chemical degradation in adverse pressure, temperature and salinity conditions (Barbara et al, 2009, Lécolier et al, 2007). American Petroleum Institute (API) had recommended eight classes of well cement Class (A to F) based on their composition, acid resistance, bearable temperature etc (Runar, 2010). Class G and H type of cements were recommended for the underground well construction. However, class G is most preferable for higher depth constructions. (Arina and Sonny, 2012). Currently 80% of oilfield wells in the world are using the Class G Portland cement for the well constructions.

Two of the most important factors affecting the integrity of well cement are salinity and temperature (Barlet et al, 2009). As we go down the earth due to the existence of various type of sub surface rock layers, the salinity varies in the range of (0- 40) % and the geothermal gradient is 30℃ /km (Barlet et al, 2010). This research focuses on the mechanical

behaviour of well cement under various curing temperature at a given salinity. There a few studies (Nasvi et al, 2012 and Lecolier et al, 2007) focusing on the behaviour of well cement with different curing temperature conditions.

Nasvi et al, (2012) compared the mechanical behavior of geopolymer and class G cement under different down-hole temperatures (20 ºC to 90 ºC). Based on the findings, it was noted that the optimum curing temperature for both class G cement for higher strength lies between 55-60 ºC. Compressive strength of class G cement initially increases and then reduces towards 80 ℃. Class G cement was identified as a good option at depth of less than 1 km (assuming a geothermal gradient of 30 ℃/km).

Lécolier et al, (2007) investigated the physical and chemical effects of supercritical CO_2 attack on well cement at different temperature (40ºC and 120ºC) and pressure (105 bar and 140 bar) conditions. When considering the effects of different temperature conditions on cement degradation by supercritical CO_2, the rate of hydration was higher at high temperature, thus greater $Ca(OH)_2$ and C-S-H was produced which may leads to the formation of greater amount of smaller unhydrated grains compared to that at the temperature 40˚C.

Major aim of this research is to study the effect of temperature (25 ºC-80 ºC) on the mechanical behaviour of well cement at 10 % of NaCl by weight of water.

2 RESEARCH METHODOLOGY

Experiments were conducted with 10 % salinity of NaCl BWOW for varying temperatures conditions of 25 ºC, 40 ºC, 60 ºC and 80 ºC. A salinity of 10 % NaCl was selected for the study, as it has been found that 10 % NaCl salinity gives the higher Uniaxial Compressive Strength values (Subaha et al, 2016).

Table 1: Composition of Ordinary Portland cement (Luke et al, 2012)

Composition	Percentage range (%)
CaO	60.2 – 66.3
SiO_2	18.6 – 23.4
Al_2O_3	2.4 – 6.3
Fe_2O_3	1.3 – 6.1
MgO	0.6 – 4.8
Others (P_2O_5, TiO_2, Na_2O, K_2O, SO_3)	Very small amount

Fig. 1: Sulphur capped sample subjecting to Uniaxial Compressive strength test.

In this study, sulphate resistance Ordinary Portland Cement samples having similar composition as class G cement sample was used as the well cement. Table 1 shows the composition of the cement used. Samples were prepared free of aggregates with a diameter of 40mm and height 80 mm using PVC moulds. The water/cement (w/c) ratio of 0.44 was used for the sample preparation. Prepared samples were kept at room temperature (25 ºC) for 12 hours, then the samples were cured at a constant salinity condition (10 % NaCl) and at different temperatures conditions for a period of 7 and 28 days.

During the air curing the top surface of the samples were covered by polythene to prevent any moisture loss from the samples. Control samples that were also kept at room temperature without brine curing was used to compare the results. For each specific condition, three samples were tested to ensure reproducibility. Figure 1 shows the cement sample subjected to uniaxial compressive strength test.

Cured samples were then Sulphur capped and were subjected to uniaxial compressive strength testing. Uniaxial compression strength testing machine available at material laboratory, Faculty of Engineering, University of Peradeniya was used to determine the uniaxial compressive strength of the samples. Scanning Electron Microscope (SEM) was used to study the microstructural variation of cement under different temperature conditions. SEM and EDX test was conducted at Geological

Department, Faculty of Science, and University of Peradeniya.

3 RESULTS AND DISCUSSIONS

Figure 2 shows the variation of compressive strength with temperature.

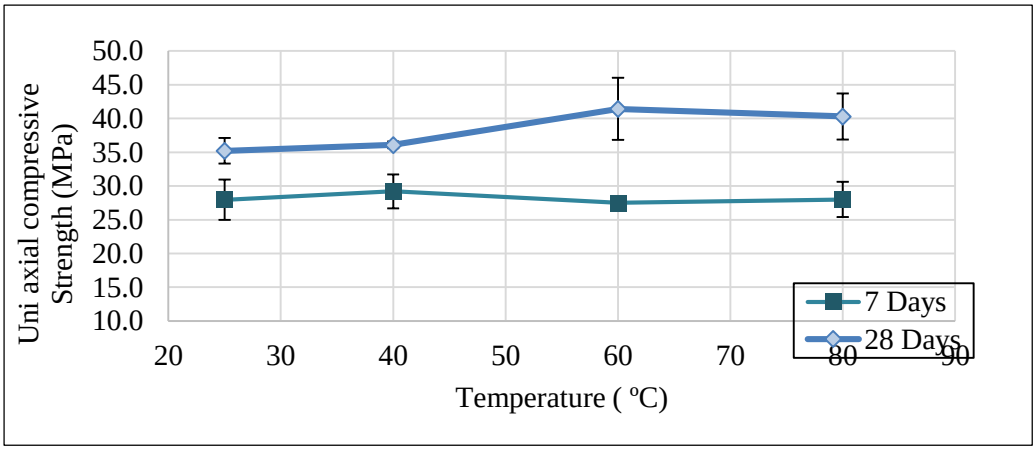

Figure 2: Variation of Uniaxial Compressive Strength with varying temperature for 7 and 28 days of curing

According to Figure 2 compressive strength for the samples cured in different temperature is shown. The uniaxial compressive strength initially increases and then decreases with temperature. For 7 days curing period, strength increases up to 40 ºC and attains peak temperature and then decreases towards 80 ºC. When the long term behavior of temperature for high strength is 60 ºC. Optimum temperature for class G cement is nearly between 50-60 ºC (Nasvi et al, 2012). With the increase of temperature the rate of hydration of well cement is considered, the optimum increases this lead to initial increase in strength, and then solubility of $Ca(OH)_2(s)$ decreases with increasing temperature. This decrease in solubility decelerates the hydration process leading to strength reduction. (Barbara et al, 2007).

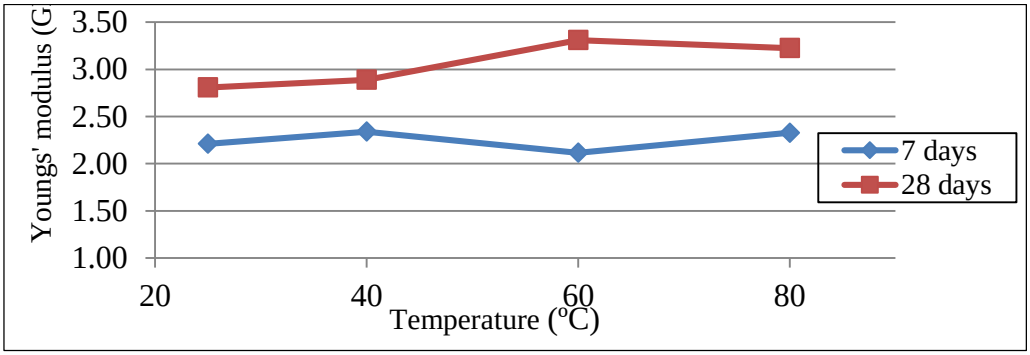

Figure 3: Variation of Young's Modulus with varying temperature for 7 and 28 days of curing

And in higher temperature C-S-H ions become denser and don't fill the capillary pores effectively. Hence at elevated temperature higher amount of Cl^- ion penetrate through cement sample and get deposited in between and causes degradation of cement sample (Arina and Sonny, 2012). Figure 3 shows the variation of Young's Modulus with varying temperature for 7 and 28 days of curing. The Young's modulus also had a similar variation as that of uniaxial compressive strength. It can be seen that stiffness of well cement increases with curing time. SEM test was conducted to study the microstructural variation of well cement with temperature. Figure 4 shows the SEM image of sample cured at a salinity of 10% NaCl saturation. Ample amount of uniformly distributed CSH-NaCl complex was found in the sample cured at 60 ºC (Figure 4 (b)) compared to the samples cured at RT and 80 ºC (Figure 4 (a) & (c)). This is due to enhanced rate of hydration at 60 ºC compared to other temperature. Highest uniaxial compressive strength values were obtained at 60 ºC is due to the uniform C-S-H products. On the

other hand, some cracks were also observed in the SEM image of the samples cured at 80 ºC and this is the reason for strength reduction towards 80 ºC. Previous studies in this regard also have showed that the strength reduces at elevated temperatures (Nasvi et al, 2012 and Mojtaba et al, 2010).

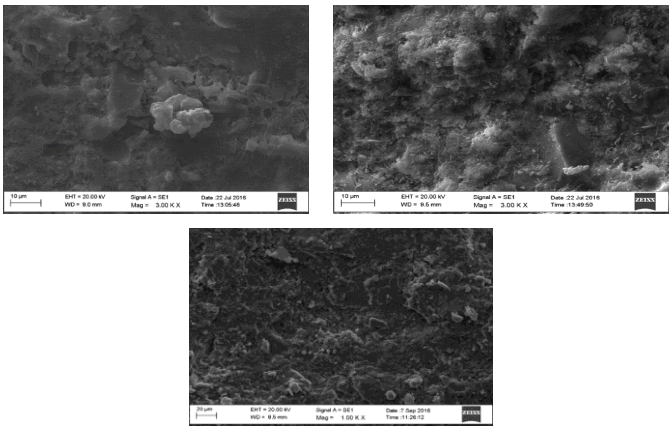

Figure 4: SEM image analysis of cement samples (a) RT 25 ºC (b) 60 ºC (c) 80 ºC

Further, Energy-Dispersive X-Ray Spectroscopy (EDX) analysis was done to ensure the traces of NaCl in cement samples. The white colour crystal forms of NaCl solid deposits were identified in the 80 ºC cement sample. It shows that in continuous ageing in brine solution, NaCl particles penetrates through the cement samples and got deposited in between and causes the degradation of the cement samples at higher temperature (80 ºC).

4 CONCLUSION

A research program was conducted to study the effect of temperature on cement samples at a constant salinity. Based on the findings of the uniaxial compressive strength of OPC samples of temperature curing at a constant salinity were found. The compressive strength initially increases with temperature up to 60 ºC towards 80 ºC and then decreases. The initial increase was due to the increased rate of hydration. In elevated temperature the C-S-H molecules becomes denser hence it cannot fill the capillary pore spaces effectively. Hence, the strength decreases with increasing temperature. The results obtained from the compressive strength were further supported by observing the microstructural variations by using Scanning Electron Microscope (SEM) and Energy Dispersive X-Ray spectroscopy analysis (EDX). These test were used to ensure that the above behavior of OPC is due to the presence of NaCl brine concentrations and its effects. On the whole the OPC Sulphate resistant well cement shows optimum strength at 60 ºC in long-term.

Journal References:

Arina B S and Sonny I. (2012). Effects of pressure and temperature on well cement degradation by supercritical CO_2, International Journal of Engineering & Technology IJET-IJENS, 10 (04): 53-61.

Barbara G, Kutchko B R, Strazisar D A, Dzombak R, Lowry, Niels T. (2007). Degradation of well cement by CO_2 under geologic sequestration conditions, Environ. Sci. Technol.
Barlet G, Rimmele G, Porcherie O, Quisel N, Desroches J. (2009). A solution against well cement degradation under CO_2 geological storage environment, International journal of greenhouse gas control 3:206–216.

Gielen D. (2003). The future role of CO_2 capture and storage, Results of the IEA-ETP model, EET/2003/04, Paris.
Lécolier E, Rivereau A, Le Saoût G, Audibert H. (2007). Durability of hardened Portland cement paste used for oil-well ementing, Oil & Gas Science and Technology Rev. IFP, 62 No. 3: 335-345.

Luke C, Deasy H, Lupton N. (2012). Integrity of Wellbore Cement in CO_2 Storage Wells State of the Art Review. Australian National Low Emissions Coal Research & Development Project 3: 1110-0084.

Nasvi M C M, Ranjith P G, Sanjayan J. (2012). Mechanical properties of geopolymer cement in brine, 7th Asian Rock Mechanics Symposium.

Nasvi M.C.M, Ranjith, P G, Sanjayan, J. (2012). Comparison of mechanical behaviors of geopolymer and class G cement as well cement at different curing temperatures for geological sequestration of carbondioxide, American Rock Mechanics Association.

Runar N R. (2010). Well Design and Well Integrity, Wabamun Area CO_2 Sequestration Project (Wasp).

Sarmiento, J L, Gruber N. (2002). Sinks for anthropogenic carbon, Physics Today: 30–36.

Geotechnical Engineering Properties of Fly Ash and Well Graded Sand Treated Peat

S. Venuja, S. Mathiluxsan
Department of Civil Engineering, University of Peradeniya, Sri Lanka

ABSTRACT: Peat is a kind of soft organic soil having partially disintegrated plant remains hence it is not good for constructions. Chemical stabilization is the commonly used ground improvement technique by adding chemical admixtures such as ordinary Portland cement, fly ash, natural fillers etc. Our research focused on stabilizing peat using a combination of fly ash and well graded sand. An experimental study was conducted to analyse the stabilization of peat with 125 kg/m^3 dosage of well graded sand and fly ash at three various proportions 10, 20 and 30 % by weight. A series of experiments including Unconfined Compressive Strength (UCS) and Rowe cell test were conducted to evaluate the compressibility behaviour of stabilized peat. UCS increases up to 10 % fly ash addition and increases with curing period for all sample types. There is an improvement in settlement behaviour of peat after the above stabilization.

1 INTRODUCTION

Peat lands cover nearly 400 million ha of earth [Bujang et al (2005)]. Low bearing capacity, high compressibility, low specific gravity, high moisture content and difficult accessibility are the main characteristics of peat [Roslan et al (2008), Kolay et al (2011)]. Peat poses serious problems in construction due to the massive primary and long term settlement when subjected to even moderate load [Roslan et al (2008)]. Hence, it is not suitable for foundations at its natural state. Peat is classified according to Von post scale system between H1 (completely fibrous peat) and H10 (completely amorphous peat) based on the degree of humification [Bujang et al (2011)].

Mechanical method and chemical method are the commonly used improvement techniques in stabilizing the soft grounds before construction. Mechanical method includes pre-loading, displacement and replacement, stone columns, vertical drains and paper drains [Bujang et al (2011), Kolay et al (2010)]. Deep mixing method is a chemical stabilization technique by adding chemical admixtures such as sand, fly ash, lime, cement, etc with peat [Bujang et al (2005), Kolay et al (2010)]. The following parts summarize the findings of studies focusing on the stabilization of peat.

Bujang et al (2005) compared the effectiveness of lime and cement on peat stabilization and found that the cement has better interaction with peat than lime because of its quick pozzolanic reactions. Roslan et al (2008) proved that the bearing capacity of stabilized peat improved by 86 % after stabilizing with cement, bentonite, sand and calcium chloride using cone penetrometer test. Kolay et al (2011) investigated the compression behaviour of peat stabilized with pond ash by conducting several unconfined compressive strength (UCS) tests. Optimum moisture content (OMC) decreases and maximum dry density (MDD) with the pond ash addition due to the consumption of pore water during the hydration process. UCS increases with the added pond ash amount as well as with the curing period due to flocculation and hydration process respectively.

Bujang et al (2011) did both experimental study using Rowe cell and numerical study using PLAXIS 2D software to find out the change in compressibility behaviour of peat stabilized with cement. They found the effect of cement is higher on sapric peat due to the higher cation exchange capacity. Kolay et al (2010) observed that 6 % and 20 % of gypsum and fly ash respectively are the optimum content that gives higher UCS values after the stabilization of peat. Ali et al (2013) conducted a study of stabilization of peat with cement and various types of natural fillers to find out the optimum filler content. They found well graded sand is the best filler giving good improvement to peat and the optimum dosage is 125 kg/m^3.

In Sri Lanka, annually 150 metric ton of fly ash is produced in Nuraicholai coal fired power plant and only about 20 % is usable for cement production, leaving huge amount of fly ash ends up in landfills. Thus in this research, chemical stabilization using a combination of fly ash and well graded sand was done. The fly ash will interact with peat soil particles and enhances the geotechnical engineering properties of raw peat. Index properties tests, UCS test and Rowe cell test were conducted to find out the improvement in compressibility behaviour of

peat after stabilization using ASTM class F fly ash and well graded sand.

2 MATERIALS AND METHODOLOGY

2.1 *Materials*

Peat sample was collected at Thorana, Kelaniya, Sri Lanka and it was like slurry. Fly ash was collected at Holcim Lanka Ltd, Puttalam, Sri Lanka. It contains more than 70 % of weight of SiO_2 + Al_2O_3 + Fe_2O_3 so that, it is classified as class F (ASTM 618). Table 1. shows the composition of fly ash used in this research. Well graded sand was collected and prepared by adding sufficient amount of particles with various sizes according to ASTM D 2487-83. It should have coefficient of uniformity (C_u) greater than 6, and coefficient of curvature (C_c) between 1 and 3. It was found that C_u is 9.23 and C_c is 1.16 for the well graded sand used in this study.

Table 1. Fly ash composition

Constituents	Percentage / (%)
SiO_2	52.03
Al_2O_3	32.31
Fe_2O_3	7.04
CaO	5.55
MgO	1.30
SO_3	0.07
K_2O	0.68
Cl	1.00

2.2 *Sample Preparation*

Due to the slurry like behaviour, peat was oven dried for two days and sieved through 4.75 mm sieve to remove the objects like roots, stones, etc. The dosage of well graded sand was fixed at 125 kg/m^3 [Ali et al (2013)]. Fly ash was added in three various proportions 10, 20 and 30 % by weight. Five different types of samples were prepared as following: (i) Raw peat (P) ; (ii) Peat + Well graded sand (PSF0) ; (iii) Peat + Well graded sand + 10 % fly ash (PSF10) ; (iv) Peat + Well graded sand + 20 % fly ash (PSF20) ; and (v) Peat + Well graded sand + 30 % fly ash (PSF30).

2.3 *Experimental procedure*

Index properties tests such as Atterberg limits test (BS1377:Part2:1990), Small Pyknometer test (BS1377:Part 2:1990) and Loss on ignition test (BS1377:Part 3:1990) were conducted in order to find out the bulk density, moisture content, specific gravity, liquid limit, plastic limit and organic content of raw peat.

Unconfined compressive strength test (BS1377:Part 3:1990) was conducted at 7 and 28 days of curing for all type of samples. A constant strain controlled loading rate of 0.7 ± 0.1 mm/min was maintained for all tests. 38 mm diameter and 76 mm depth samples were prepared and allowed for air curing. At least two samples were tested and average results were taken as UCS values. Samples also tested to find out UCS values immediately after preparation as control samples. Fig. 1 shows the UCS samples at air curing stage and Fig. 2 shows the UCS apparatus with loaded peat sample.

Fig. 1 Air curing of UCS samples

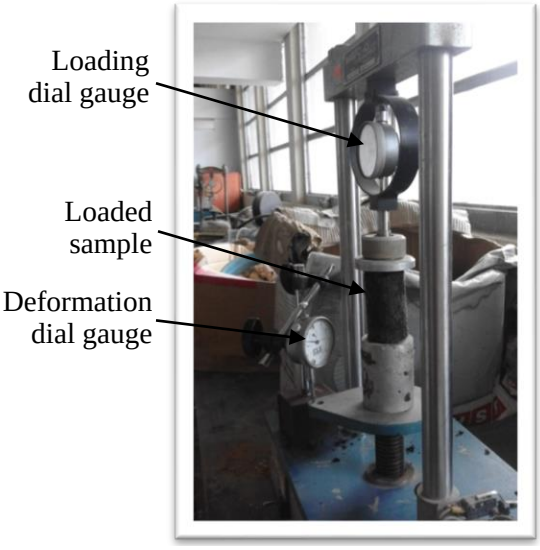

Fig. 2 UCS apparatus

In Rowe cell test, equal strain condition was maintained and one-way top vertical drainage was allowed. The sample size was 151.8 mm diameter and 50 mm depth. The applied consolidation pressures were 50, 100 and 200 kPa. First, de-aired water was poured at the base and porous plate was inserted. Then the sample was placed on the porous plate. After pouring some de-aired water on the top surface of the sample, filter paper was laid on it. Diaphragm balloon was partially filled with water and positioned on top of the filter paper. All bolts and nuts were fixed simultaneously. Dial gauge was set vertically to readout the settlement of the sample. Diaphragm balloon was filled with water completely. The diaphragm pressure line, the drainage line and the pore pressure transducer were connected to the Rowe cell apparatus. Fig. 3 shows the Rowe cell testing apparatus.

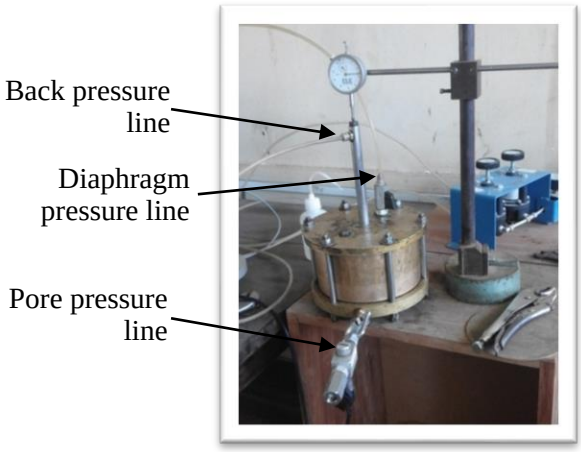

Fig. 3 Rowe cell apparatus

Initially, 10 kPa back pressure was applied to the sample and waited until the pore pressure reaches to 10 kPa to ensure the completion of the saturation. Then the drainage valve was closed and 50 kPa diaphragm pressure was applied. Dial gauge was set to zero after the increase in pore pressure equals the applied diaphragm pressure. Drainage valve was then opened and stop watch was activated simultaneously. The dial gauge reading and the pore pressure reading were taken with corresponding time. These procedures were repeated for other two diaphragm pressure values (100 kPa and 200 kPa).

3 RESULTS AND DISCUSSION

3.1 *Index properties of raw peat*

Based on the tests conducted, raw peat has the following properties: bulk density of 1055 kg/m^3, moisture content of 102 %, specific gravity of 1.90, organic content of 83.7 %, liquid limit of 101.2 % and non-plastic. Based on these results, peat is classified as amorphous peat [Youventharan et al (2007), Sina et al (2011)].

3.2 *UCS results*

Figure 3 shows the UCS test results. UCS increases with curing period for all types of sample, due to the pore water consumption is high as fly ash particles produce cementing materials throughout the hydration process [Kolay et al (2011)]. There is an initial increase in UCS up to 10 % fly ash addition, because of the air voids in peat were filled with finer fly ash particles [Kolay et al (2011)]. UCS reduces as more fly ash added to the mix. This is due to the un-reacted fly ash particles in the mix [Kolay et al (2011)]. From these results, it is found that the optimum mix proportion of fly ash is 10 % that gives good compressibility behaviour improvement to raw peat.

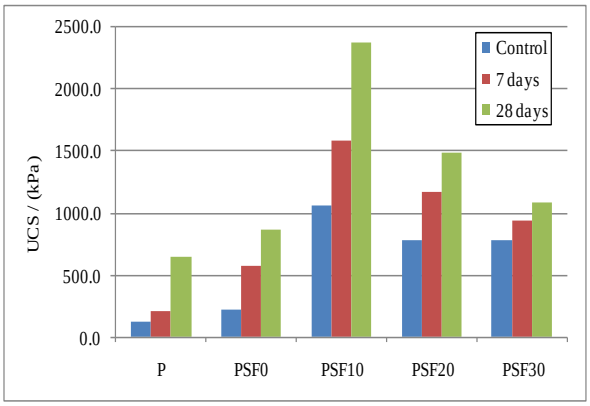

Fig. 4 UCS test results

3.3 *Settlement behavior*

Rowe cell test was conducted for raw peat and the peat stabilized with 10 % fly ash content which gives the highest UCS. Fig. 4 shows the settlement variation with time of both samples with various consolidation pressures. There is more than 50 % settlement reduction after stabilization of peat using 10 % fly ash and well graded sand for all consolidation pressures. Therefore, the settlement behaviour of peat improved after the stabilization. Fig. 5 shows the variation of void ration with the applied consolidation pressure for both samples. From the slope of these curves, compression index (C_c) of peat and stabilized peat with 10 % fly ash were obtained [Eq.(1)]. Compression index of raw peat was 0.548 and stabilized peat with 10 % fly ash was 0.149. There is no secondary consolidation after the stabilization. It shows the improvement in the compressibility parameters after stabilization

and it is due to the flocculation of fly ash particles with soil particles [Phanikumar (2009)].

$$C_c = (e_2 - e_1) / \log (p_2/p_1) \qquad (1)$$

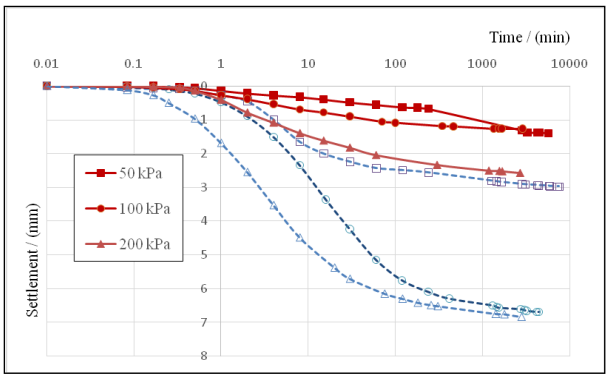

Fig. 4 Settlement variation with time of raw peat (hollow line) and stabilized peat with 10 % fly ash (solid line)

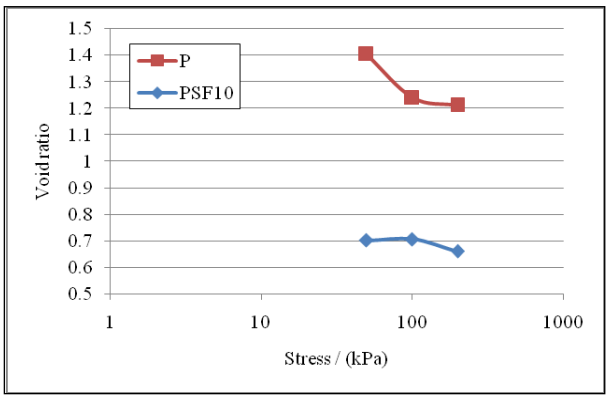

Fig. 5 Variation of void ratio with stress

4 CONCLUSIONS

In order to study the compressibility behaviour of stabilized peat with ASTM class F fly ash (0 - 30 % by weight) and well graded sand (125 kg/m^3), an experimentally based study was conducted. The following conclusions were made. The type of peat used in this research is amorphous. The optimum mix composition is peat + well graded sand + 10 % fly ash, as it gave the highest UCS value. The UCS of stabilized peat with 10 % fly ash was nearly 7 times of the UCS of raw peat. UCS also increased with the curing period. Based on Rowe cell test results, it is found that there is an improvement in compressibility behaviour and consolidation parameters after the stabilization of peat using class F fly ash and well graded sand. On the whole, this study results may be used in improvement of peat lands using deep mixing method. Fly ash may be added in powdered form into peat soil by dry mixing method since peat has high water content.

ACKNOWLEDGMENTS

We would like to thank all people who helped us to successfully complete our research. Especially, we wish to thank Dr.M.C.M.Nasvi (Lecturer of Civil Engineering, Department of Civil Engineering, University of Peradeniya, Sri Lanka), our project supervisor, who gave guidance and support in developing ideas on this research.

REFERENCES

Ali D, Kamarudin A, Nazri A 2013. Influence of natural fillers on shear strength of cement treated peat: GRADEVINAR 65, Vol 7, 633-640.

Bujang B.K.H, Shukri M, Thamer A.M 2005. Effect of Chemical Admixtures on the Engineering Properties of Tropical Peat Soils: American Journal of Applied Sciences 2, Vol 7, 1113-1120.

Bujang B.K.H, Sina K, Arun P, Maassoumeh B 2011. A study of the compressibility behavior of peat stabilized by DMM: Lab Model and FE analysis: Scientific Research and Essays, Vol 6(1), 196-204.

Kolay P.K, Pui M.P 2010. Peat Stabilization using Gypsum and Fly Ash: UNIMAS E-Journal of Civil Engineering, Vol 1.

Kolay P.K, Sii H.Y, Taib S.N.L 2011. Tropical Peat Soil Stabilization using Class F Pond Ash from Coal Fired Power Plant: International Journal of Civil and Environmental Engineering 3, Vol 2, 79-83.

Phanikumar B.R 2009. Effect of lime and fly ash on swell, consolidation and shear strength characteristics of expansive soils: a comparative study: Geomechanics and Geoengineering, Vol 4(2), 175-181.

Roslan H, Shahidul I 2008. Properties of Stabilized Peat by Soil-Cement Column Method: Bund. J, Vol 13.

Sina K, Arun P, Bujang B.K.H, Jafar B.B, Farah N.A, Abdul A, Mohammad A 2011. Influence of Cement – Sodium Silicate Grout Admixed with Calcium Chloride and Kaolinite on Sapric Peat: Journal of civil engineering and management, Vol 17(3), 309-318.

Youventharan D, Bujang B.K.H, Azlan A.A 2007. Engineering Properties and Compressibility Behavior of Tropical Peat Soil: American Journal of Applied Sciences 4, Vol 10, 768-773.

Numerical Analysis of Geomat Reinforced Vertical Earth Embankments Using Plaxis Software

G. Yasotharan and S. Kugaruban
Department of Civil Engineering, University of Peradeniya, Peradeniya, SriLanka.

ABSTRACT: The design procedure of reinforced earth retaining structures considers the safety against tensile failure and pull out failure as the internal stability criteria. However, evaluation of the lateral deformation also needs to be considered as an important criterion to satisfy serviceability limit states. It is imperative that the designer limits the lateral deformation of reinforced earth walls under service loads. In a reported number of previous studies, extensive laboratory experiments have been carried out to investigate the lateral deformation characteristic of embankments reinforced with coir mats. For this purpose, ordinary coir mats and those coated with polyethylene to improve their durability under acidic and alkaline environments have been used. The above studies, also investigated the effect of wetting on the lateral deformation as well. In this study, numerical analyses of the above laboratory experiments are carried out using Plaxis 2D software to determine lateral deformation characteristics and the results are compared with the experimental results. The analyses was carried for uncoated and coated geomats used to reinforce a vertical embankment prepared to 95% of maximum dry density and that subjected to soaked conditions which simulates exposure to rainy weather.

The results show that the variations of lateral deformation obtained from the numerical analyses under various conditions are similar to those observed in the experimental studies. However, quantitatively, the lateral deformation obtained from the numerical analyses show less value in magnitude than those observed in the experimental work.

1 INTRODUCTION

In civil engineering applications, embankments are constructed to support road or railway running through low lying areas, in canal excavations, dams and also in maintaining two different elevations as in retaining structures. These embankments are mainly built using compacted reinforced or unreinforced soil and with or without a rock fill, or even using mass concrete. Selection of material not only depends on the side slope of the embankment, the geometry and its dimensions but also the sub-grade soil type.

In case of vertical embankments a supporting structure needs to be provided to withstand lateral earth pressures. However, use of polymer georeinforcement to support the embankment internally would eliminate the need for an external structure. Instead, it is also possible to use geomats made of coir as the reinforcing material (as a cost effective solution to stabilize the vertical face of an embankment making use of its engineering properties, taking care of the durability considerations of coir mats against degradation by coating with a polymer (eg.Polythene). Retaining structures are usually designed to take care of ultimate limit states (ULS) (Chai and Zhu, 2002). However, it is also important to ensure that serviceability limit states are also satisfied, an essential requirement for its satisfactory functionality.

Jayaprakash et.al (2012) carried out laboratory model studies to compare the performance of the coated and uncoated Geomat reinforced vertical embankments.

In this research, a numerical analysis is carried out to investigate the deformability of Geomat reinforced vertical embankments. The methodology involved validation of the numerical model against experimental records from past studies.

2 LITERATURE REVIEW

Reinforcing the soil is the common method used to improve the stability of an embankment so that external supporting system is not required. When reinforcements are placed at a designed vertical spacing, each of reinforcement will carry the force transferred by the soil within its tributary area which can be calculated using Rankine's active earth pressure theory. It is also possible to use coir geomats as the reinforcing material as a cost effective solution to stabilize the vertical face of an embankment making use of its engineering properties [Kurukulasuriya et.al, 2011].

Krishanthan et al, (2011) had conducted an experimental study to investigate the suitability of

coir geomats in an internally stabilized vertical embankment construction. They constructed an embankment of 500 mm in height, 605 mm in width, and 700 mm in length with five layers of reinforcement and then the embankment was loaded under dry and wet conditions.

Based on the laboratory experimental model study, they concluded that the lateral displacement in both reinforced embankments increased with the applied pressure and decreased with depth and whether the loading is applied under natural moisture content of the fill or under soaked conditions and from the results, coir geomat reinforced vertical wall showed less lateral deformation than the geotextile reinforced wall, at the same fraction of the allowable surcharge pressure corresponding to each material.

Jayaprakas et al, (2012) had conducted a research that investigates the suitability of coated coir geomat as a reinforcement considering lateral displacements. The suitability of durability improved coir geomat, made by coating coir geomat with waste plastic material as reinforcement material, for satisfying lateral displacement was determined by laboratory model tests. For this study, they used the same soil and experimental setup used in a study by Krishanthan et al. (2011) which made it possible to carryout comparative studies on the suitability of durability improved coated coir geomat.

Based on the laboratory experimental model study, they came to a conclusion that whether the loading is applied under dry or wet conditions, the durability improved coated coir geomat reinforced vertical wall showed similar lateral deformation to that of uncoated coir geomat reinforced wall. Therefore, the improvement of the durability by coating a waste polymer material did not affect the lateral deformation characteristics of a coir geomat reinforced vertical wall.

Chai et al, (2002) had conducted numerical analyses and concluded that only when the embankment approaches to failure, the reinforcement has noticeable effect on the lateral displacement of the soil.

3 METHODOLOGY

3.1 *Parametric Study*

Several parametric studies were carried out to investigate the effect of various parameters on the lateral deformation of earth embankments using Plaxis software.

- Embankment with different side slope
- Embankment with and without reinforcement
- With different reinforcement spacing
- Embankment analyses in different scales.

3.2 *Experimental Data collection*

Material properties (Table 1) required for the numerical analyses and experimental results needed for comparison and validation were collected from the past studies of Kurukulasuriya (2011) and Jayaprakas (2012).

Table 1. Material properties from the past studies

Material		Parameter	Value
Silty Sand		c′	5 kPa
		ϕ′	31°
		γ_{sat}	20 kN/m^3
		γ_{unsat}	17 kN/m^3
		E	20 MPa
		ν	0.4
		k	25 m/day
Geomat	Uncoated	EA	5.2 kN/m
	Coated		7.4 kN/m

3.3 *Numerical Analysis*

The same material properties and boundary conditions applicable to past experimental studies were used to construct the geometry model for the numerical analyses. For this study, Mohr-Coulomb model was used as the material model and the use of uncoated and coated geomats in a vertical embankment were analyzed under dry and wet conditions where the values of material unit weight and interface shear strength between soil and geomat were considered to be affected by the moisture content of the embankment as given in Table 2.

Table 2. Parameters used in Plaxis software for dry and wet condition

Parameter	Dry condition	Wet Condition
γ_{sat} (kN/m^3)	20.0	20.0
γ_{unsat}(kN/m^3)	17.0	20.0
Interface strength	1.00	0.65

The experimental set up of the vertical embankment used in previous studies was modelled in Plaxis software as shown in Fig. 1 with geomats reinforcement placed at the same location as was placed in the experimental set up and 15 noded triangular finite element mesh used.

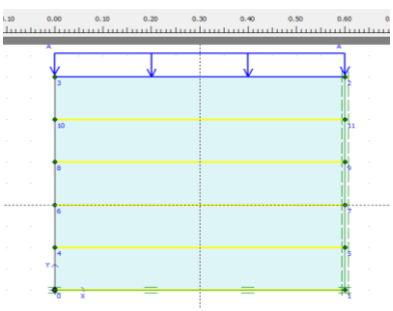

Fig. 1 Generated Material model

Gradually increasing surcharge loading was applied to the model and deformations were calculated for each loading.

4 RESULTS

4.1 *Comparison of numerical and experimental results*

Lateral and vertical deformations obtained experimentally and numerically under different loading were plotted as described below.

- Uncoated geomat under dry condition

Fig.2 shows the experimentally and numerically obtained profiles of the vertical face of the vertical embankment after deformation depicting the extent of the lateral deformation when the top surface was subjected to three different values of surcharge pressure

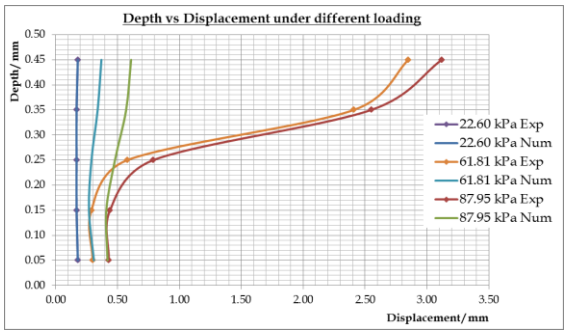

Fig. 2Comparison of results for uncoated geomat under dry condition

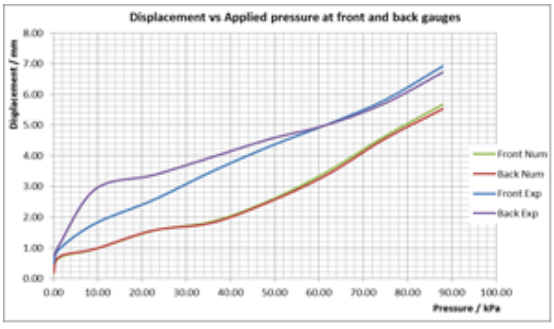

Fig. 3Comparison of vertical displacement with depth for uncoated geomat

Comparison of horizontal displacement with depth shows that the variation between experimentally and numerically obtained profiles is similar at early stages of loading. However, comparison of vertical displacement with depth (Fig.3) shows similar variation for both experimental and numerical analyses. But, quantitatively, the displacements obtained from the numerical analyses show less value in magnitude than those observed in the experimental work.

- Coated geomat under dry condition

Similar comparison of experimental and numerical results of lateral and vertical deformations of vertical embankment reinforced with coated geomats is given in Fig.4 and 5 respectively.

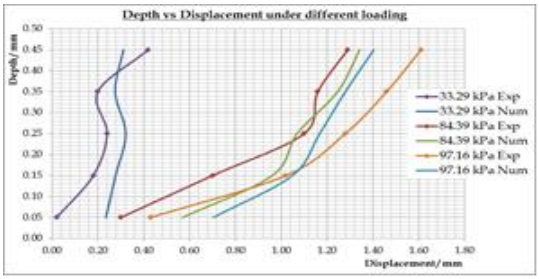

Fig. 4Comparison of results of lateral deformation for coated geomat under dry condition

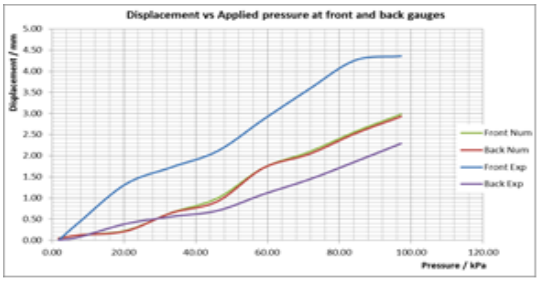

Fig. 5Comparison of vertical displacement with depth for coated geomat

- Uncoated geomat under wet condition

The experimental and numerical results of deformation characteristics for uncoated geomat reinforced vertical embankment under wet conditions is shown in Fig.6 and 7 respectively.

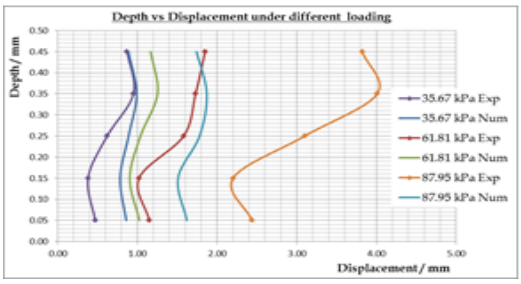

Fig. 6Comparison of results for uncoated geomat under wet condition

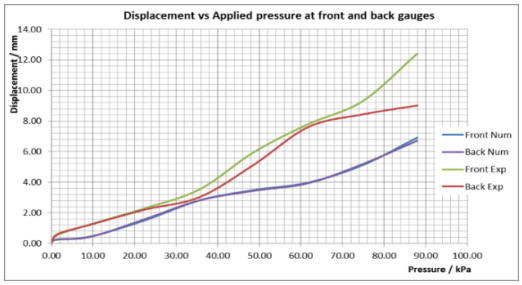

Fig. 7Comparison of vertical displacement with depth for uncoated geomat

- Coated geomat under wet condition

Comparison of horizontal displacement with depth (Fig.8) shows that the variation is similar to each other. However, the comparison of vertical displacement with depth (Fig.9) for both experimental and numerical analysis show greater deformation in the experiment than that in the numerical analysis

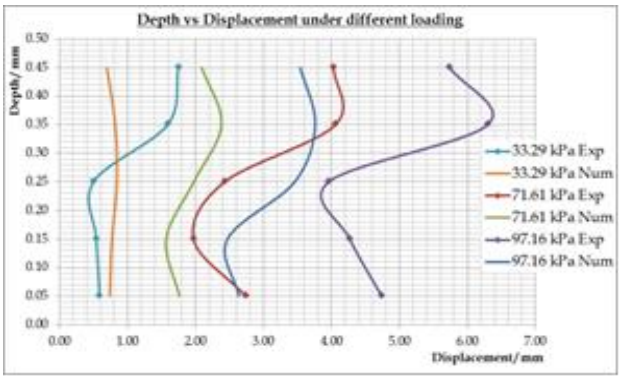

Fig. 8Comparison of results for coated geomat under wet condition

This may have been caused due to loosening of soil near the top surface during the soaking stage.

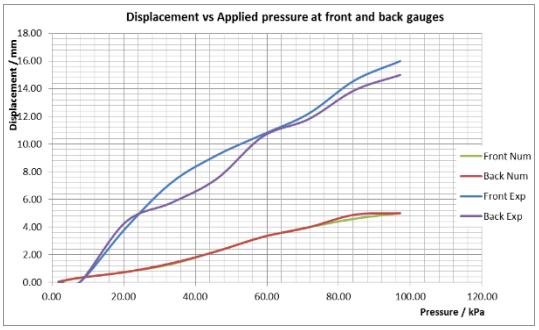

Fig. 9Comparison of vertical displacement with depth for coated geomat

4.2 *Development of plastic zone*

The Plastic point option available in the Plaxis software shows the stress points that are in a plastic state, displayed in a plot of the undeformed geometry. Plastic points can be shown in the 2D mesh or in the elements around a cross section. The plastic stress points are indicated by small symbols that can have different shapes and colours, depending on the type of plasticity that has occurred where a red square indicates that the stresses lie on the surface of the Coulomb failure envelope and a white cube indicates that the tension cut-off criterion has been reached.

The Mohr-Coulomb plastic points are particularly useful to check the failure plane. In this numerical analysis a surcharge pressure of 100 kPa was applied and the plot of plastic points in the undeformed geometry was extracted. Fig. 11 shows the plot of plastic points that are on the Mohr-Coulomb failure surface defined by the shear strength parameters, under an applied surcharge pressure of 100 kPa. The development of plastic points appear to show a failure surface similar to that is developed in a slope failure. However, this kind of a failure mechanism may not be possible in the experimental set up as the loading was carried out through a rigid steel plate. However, in the experimental set up, a greater vertical deformation observed at the front gives an indication that yielding may have taken place towards the front as indicated in the numerical analysis.

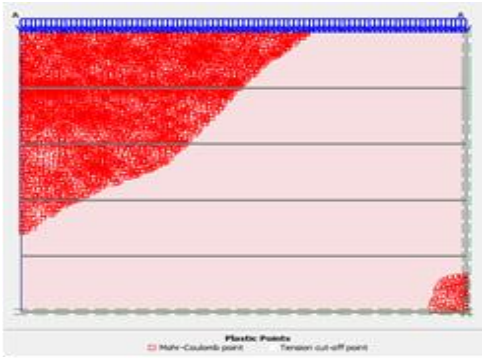

Fig. 10 Plot of plastic points in theundeformed geometry under a surchargepressure of 100 kPa

5 CONCLUSIONS

A numerical analysis was carried out to investigate the comparability of the lateral and vertical deformation characteristics of a coated and uncoated geomat reinforced vertical embankment under dry and wet conditions with the results of an experimental investigation.

The comparison of experimental and numerical results indicated that variations of the lateral and vertical deformations obtained from numerical analyses were similar to those of experimental work. However, quantitatively the deformations obtained from the numerical analyses show lesser values in magnitude than those observed in the experimental work.

REFERENCES

Jayaprakash B., Mahotharan K., Manoj L. and Kurukulasuriya L.C., 2012. Durability Improved Geomat Reinforced Vertical Embankment Behaviour, Proceedings, Peradeniya University Research Sessions 2012.

ChaiJ.C. and Zhu H.H., 2002. Behaviour of reinforced embankment over soft subsoil, Proceedings of international seminar on practice and advance in geotechnical engineering, Shanghai, China.

KurukulasuriyaL.C., Mahinthakumar N., TheenathayarlT. and Krishanthan T., 2011. Lateral Deformation Characteristics of Coir Geomat Reinforced Vertical Embankments, Proceedings, International Conference on Structural Engineering, Construction and Management, Kandy, Sri Lanka